

Evidence for shear failure in forming near-equatorial lineae on Europa

Nicole A. Spaun¹

Department of Geological Sciences, Brown University, Providence, Rhode Island, USA

Robert T. Pappalardo

Astrophysical and Planetary Sciences Department, LASP, University of Colorado, Boulder, Colorado, USA

James W. Head

Department of Geological Sciences, Brown University, Providence, Rhode Island, USA

Received 9 April 2001; revised 21 January 2003; accepted 26 February 2003; published 21 June 2003.

[1] Global stress models for Europa are unable to readily explain the orientations of lineae in the equatorial region of Europa's trailing hemisphere if lineae originate as tension cracks. Our analysis of two equatorial, trailing regions reveals that lineae are predominantly oriented NE and NW, and E-W lineae are rare, contrary to predictions of stress and formation models. The measured orientations are consistent with an origin by shear failure. The studied regions are located near the point of maximum differential stress and minimum surface tensile stresses, where shear faulting may surmount tension fracturing. Several types of lineae are recognized; their relative abundance is inferred to have changed with time, consistent with formation models suggesting lineae evolve from simple troughs to complex ridges. The opening of crevasse-like tensile fractures is not required for generation of all lineae; the observations are consistent with ridge formation models where troughs (formed in tension or shear) experience shear heating from tidal deformation, allowing warm ice to buoyantly uplift, creating ridges. The stratigraphic relationships indicate the following: ridged plains formed first, followed by continued formation of a wide range of lineae, and lastly emplacement of lenticulae and continued lineae formation. This sequence is consistent with an early thin, brittle lithosphere that thickened with time and was subject to repetitive diurnal tides during $\sim 30^\circ$ – 90° of nonsynchronous rotation. Ultimately, the thickened shell underwent thermally induced solid-state convection, producing lenticulae. The young surface age of Europa implies that this entire stratigraphic sequence was emplaced in the geologically recent past. *INDEX*

TERMS: 6218 Planetology: Solar System Objects: Jovian satellites; 5475 Planetology: Solid Surface Planets: Tectonics (8149); 5470 Planetology: Solid Surface Planets: Surface materials and properties; 5430

Planetology: Solid Surface Planets: Interiors (8147); 5418 Planetology: Solid Surface Planets: Heat flow;

KEYWORDS: Icy satellites, Jovian satellites, Europa, surface geology, tidal stresses, tectonic processes

Citation: Spaun, N. A., R. T. Pappalardo, and J. W. Head, Evidence for shear failure in forming near-equatorial lineae on Europa, *J. Geophys. Res.*, 108(E6), 5060, doi:10.1029/2001JE001499, 2003.

1. Introduction

[2] Europa's icy surface is criss-crossed by long, linear troughs and ridges, collectively known as lineae. Global stress models have been developed to explain the potential forces affecting the European ice shell and surface; these models are tested by analyses such as the study of the orientations of lineae [e.g., Helfenstein and Parmentier, 1980; McEwen, 1986]. The stresses generated on Europa by nonsynchronous rotation and diurnal tides have been

suggested to create the tectonic lineae [e.g., McEwen, 1986; Greenberg *et al.*, 1998]. The orientations of lineae should thus reveal the record of the changing stress patterns across the ice shell. Previously many of these models have had particular difficulty in explaining the observed orientations and intersection angles of lineae near Europa's equator on the trailing quadrant if these lineae open as tensile fractures [e.g., Leith and McKinnon, 1996; Greenberg *et al.*, 1998]. Tensile fractures would open orthogonal to the least compressive stress, which should generate mostly east–west oriented lineae near Europa's equator. However the images show abundances of lineae oriented northeast and northwest with high intersection angles. To document the region's geology and evaluate potential stress models, we have used Galileo images to

¹Now at NASA Ames Research Center, Moffett Field, California, USA.

perform detailed geological mapping of two areas within the trailing hemisphere of Europa.

[3] During the fourth Jovian orbit of the Galileo mission (orbit E4), images near (5°N , 327°W) were obtained at ~ 25 meters/pixel resolution (henceforth called the “E4 region”) (Figure 1). This region was also imaged at a resolution of ~ 600 m/pxl by Galileo for context. The context reveals the general nature of this area, but shows little detail. The E4 mosaic of images (Figure 2) was analyzed by constructing a geological map (Figure 3a) illustrating the basic geological units and structures and their relationships. Synthesis of the map yields insights regarding the inferred modes of formation for this area.

[4] Also during orbit E4, images of an area now known as Conamara Chaos were taken at a resolution of 1.2 km/pixel. The area was then targeted during the sixth orbit (E6) to obtain images at a resolution of ~ 180 m/pixel. We mapped an area (Figures 1, 3b, and 4) centered at (14°N , 271°W) for detailed analysis (henceforth called the, “E6 region”) [Spaun *et al.*, 1998a]. Examination of the geological map of the E6 region (Figure 3b), like that of the E4 region, reveals the local geology and indicates the geological history typical of this region.

[5] Our work addresses critical questions about the nature of Europa’s surface features, specifically in the equatorial trailing region. Do lineae evolve from troughs to ridges? What are the orientations of lineae within this region, and what are the implications for the local and global stress history? By what means did lineae form within this quadrant of Europa, and what are the implications for ridge formation in general? What is the stratigraphic record in the studied regions and what does this imply for the origin and evolution of Europa?

2. Geological Structures, Features, and Units

[6] Geological mapping of the selected regions (Figures 1, 3, and 4) reveals the presence of two main types of structures and features, lineae (Figure 5) and lenticulae (Figure 6), and one major geologic unit, ridged plains (Pr, Figure 5). We describe each of these in detail and then examine their stratigraphic relationships.

2.1. Ridged Plains

[7] Ridged plains (Pr, white) consist of sections of the mapped regions with multiple crosscutting ridges and troughs that have parallel, subparallel, and multiple orientations [Greeley *et al.*, 1998, 2000]. These regions are characterized by a high density of relatively old linear features of short length that cross-cut and modify each other to such an extent that the sequence of ridge emplacement and modification is ambiguous. The unit may represent our inability to recognize and map discrete older lineae and features as they become more dissected and segmented with time, or the ridged plains could have formed by a distinct process or processes. The orientations of the linear segments in the ridged plains are similar to the trends of the regional lineae (see section 2.2) and therefore the same stress regimes are likely to have influenced the formation of both lineae and ridged plains.

[8] Within the western section of the E4 high-resolution region, a subset of the ridged plains unit is observed: Wash-

Board Plains (Pwb, light purple). These convex ridges and troughs are characterized by small (150 m–300 m wide) N-S oriented single ridges that fork along their trend without cross-cutting one another. The washboard ridges are bounded, and apparently terminated, by more recent lineae of various morphological types. There are no obvious examples of this unit elsewhere. As the unit is abutted at all contacts by recent lineae this suggests that the washboard plains are of limited extent. The washboard plains unit has not been identified in the E6 region; when re-sampling the E4 high-resolution images to match the lower resolution of the E6 images, it is apparent that identification of the washboard plains as a distinct part of ridged plains is challenging.

2.2. Lineae

[9] The most prominent structures in the mapped areas are a series of linear features (lineae) at various scales and orientations criss-crossing the region. Such features, described by Lucchitta and Soderblom [1982] from Voyager data, typically cross Europa’s bright lineated plains. Higher resolution Galileo imaging has shown these lineae to be both troughs and ridges [Greeley *et al.*, 1998]. Detailed descriptions of the linea types revealed by Galileo data have been made by Geissler *et al.* [1998a], Greenberg *et al.* [1998], Pappalardo *et al.* [1998b], and Head *et al.* [1998a, 1999]. We employ the classification scheme shown in Figure 5 [Pappalardo *et al.*, 1998b; Head *et al.*, 1999]. The classes closely resemble those of Greenberg *et al.* [1998]; however, the Pappalardo *et al.* [1998b] linea classes are more detailed and are not tied to a particular mechanism of ridge formation. We assess the distribution, orientation, and stratigraphic relationships of all the prominent lineae in the mapped area. The linea classes are as follows:

2.2.1. Isolated Troughs (Ti; Red)

[10] These are narrow, individual linear depressions without significant raised rims. Isolated troughs in the mapped regions commonly range from ~ 75 m to ~ 350 m in width and are generally >50 km in length, commonly extending completely across the mapped regions. Isolated troughs are interpreted to represent fracturing or faulting, possible mass wasting of the slopes, and no subsequent deformation. Isolated troughs as mapped are much more abundant in the E4 region than in the E6 area (Figure 5); this is most likely due to the higher resolution of the E4 images, which allows for better recognition of such narrow features.

2.2.2. Raised-Flank Troughs (Trf; Orange)

[11] Up to several hundred meters wide, raised flank troughs are characterized by a narrow central trough and immature or poorly developed raised rims. Like (Ti) they are linear and may extend for many tens of kilometers and resemble isolated troughs with raised flanks. We infer that (Trf) may have initially formed in a manner similar to (Ti), with an associated process that acted to create or raise the flanks (such as flexure from linear diapirism [Head *et al.*, 1999; Gaidos and Nimmo, 2000], dike intrusions [Turtle *et al.*, 1998], tidal pumping of liquid [Geissler *et al.*, 1998a; Greenberg *et al.*, 1998], or pyroclastic volcanism [Kadel *et al.*, 1998]).

2.2.3. Double Ridges (Rd; Yellow)

[12] Double ridges are composed of two parallel ridges of positive topography and occur as both prominent individual

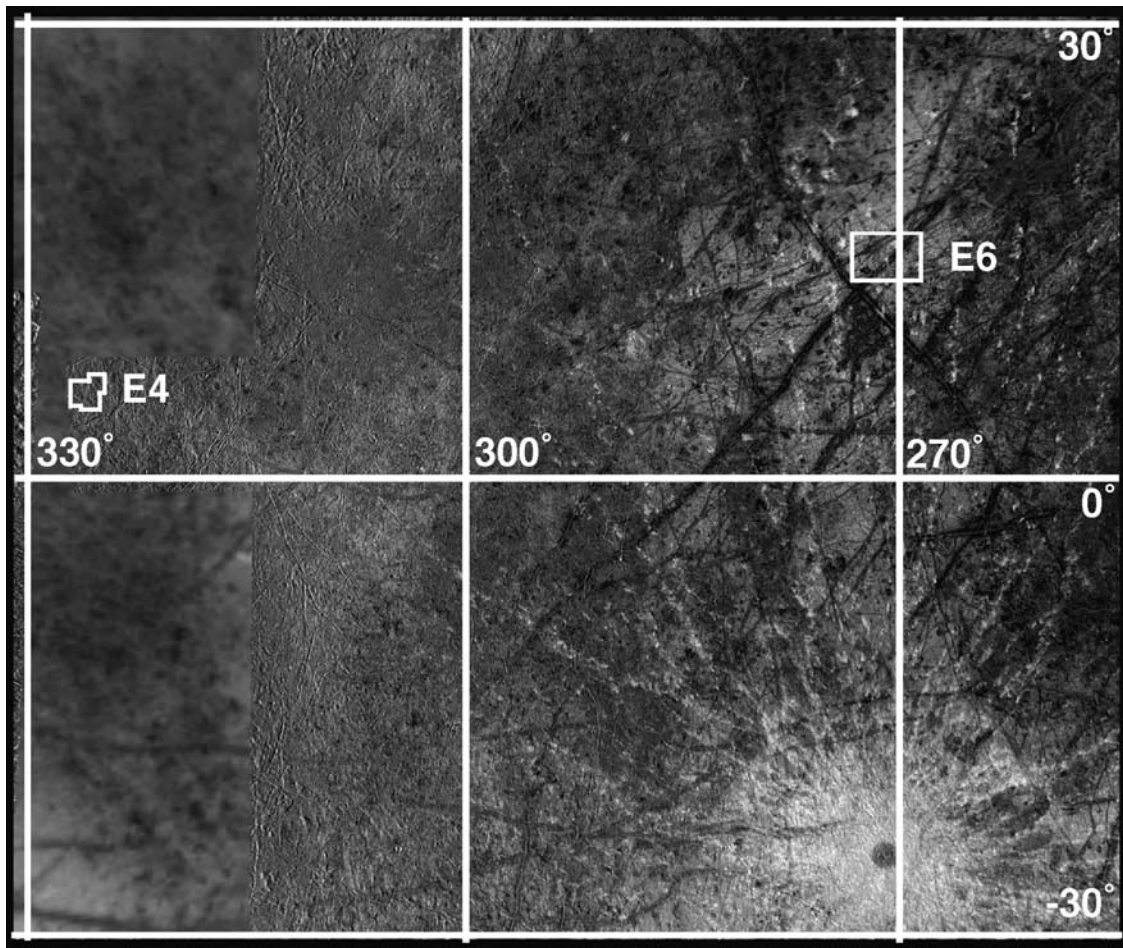


Figure 1. Context image indicating the locations of the selected areas of study, the E4 and E6 regions. White boxes indicate the locations and approximate sizes of the mapped regions.

ridges and short dissected components of the ridged plains (Pr). They range from a few hundred meters to ~ 2 km wide in these regions, and can extend for up to tens of kilometers in length. The ridges tend to be linear and fairly uniform over their extent, suggesting a process similar to that forming Trf where flanks of preexisting cracks are further amplified, possibly by one or more of the processes listed above. Although distinctive, these features can be difficult to distinguish from raised-flank troughs at certain orientations and illumination geometries, especially at the lower resolution of the E6 mapped region; thus, we estimate that as many as 20% of the lineae in these classes may belong in the other respective group. Double ridges and raised-flank troughs occur with a similar high abundance in both regions (Figure 5). There is a nearly continuous range of features between the isolated troughs (Ti) and the double ridges (Rd), with raised-flank troughs (Trf) in the transition; the close relation of these ridges supports a continuum of ridge classes as suggested by the models of Pappalardo *et al.* [1998b] and Greenberg *et al.* [1998].

2.2.4. Triple Ridges (Rt; Green)

[13] Triple ridges are comprised of three subparallel ridges separated by two troughs [Pappalardo *et al.*, 1998b]; these are rare in both of the mapped areas. These ridges range from ~ 600 m to ~ 2 km in width and extend for a few tens of kilometers.

2.2.5. Medial Trough Ridges (Rmt; Blue)

[14] These ridges have a central trough, resembling a Ti, surrounded by smoother material and bounded by narrow depressions or ridges. This morphology resembles features called bands [Prockter *et al.*, 1999; Greeley *et al.*, 2000]; however the definition of band material involves an albedo contrast that is not apparent in these images. Only a few of these ridges are observed in either mapped area. We infer that these ridges also have been formed by extrusion, intrusion, or a combination of these factors.

2.2.6. Complex Ridges (Rc; Purple)

[15] This unit is a broad category that includes any lineae structurally more complex than a triple ridge. They generally have multiple parallel ridges and troughs, and some examples have a cusate medial trough. A few complex ridges resemble “bands” though the internal texture and morphology of bands is generally much smoother and more symmetric. Complex ridges in the mapped regions range from 1.5 km to 4 km in width. Complex ridges are the most abundant linea type found in the E6 mapped area, while they are rare in the E4 region; this is most likely due to the smaller area of the E4 region and possibly the higher resolution of the images allowing for finer distinction between ridge units.

2.2.7. Unclassified Lineae (Unc; Brown)

[16] These lineae are unable to be confidently resolved into specific trough or ridge morphological types due to the

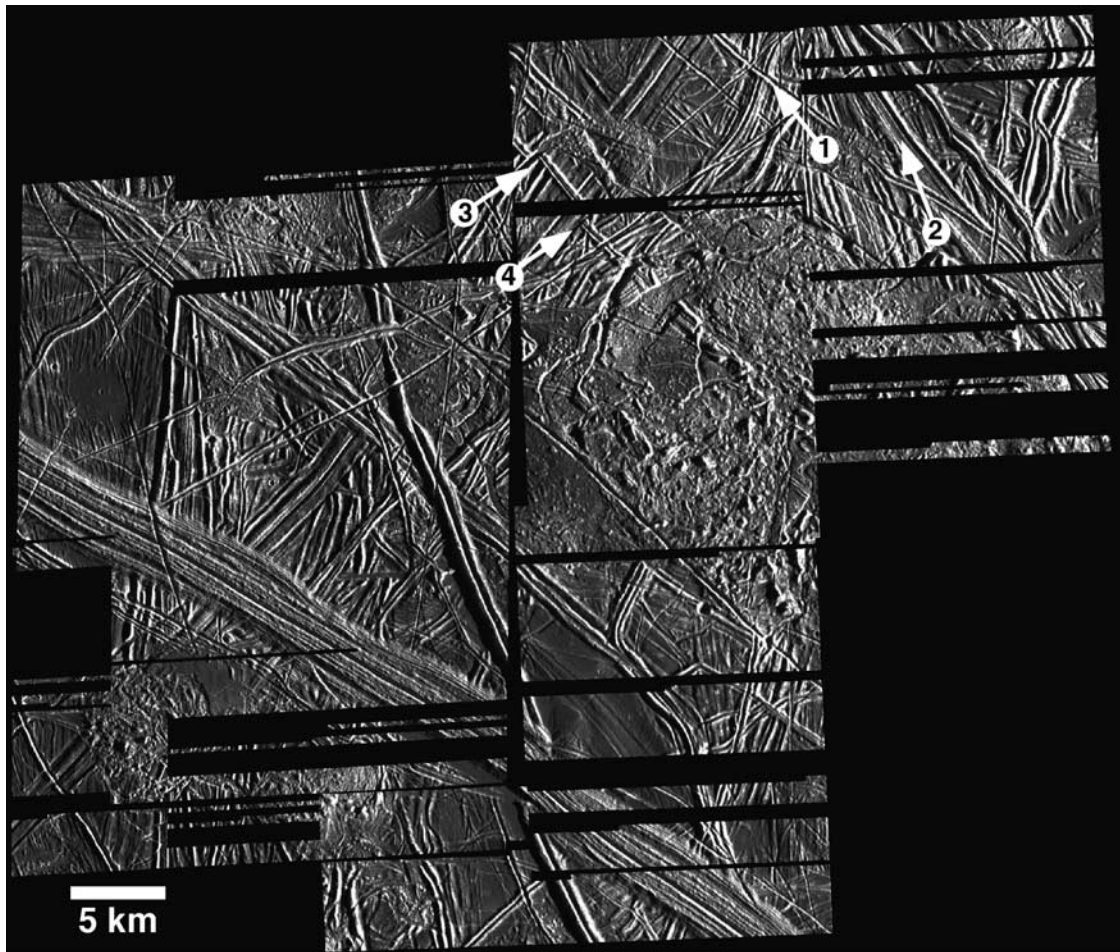


Figure 2. Mercator reprojected image mosaic of the E4 region of mottled terrain. Five images form this mosaic, centered at (5°N , 327°W) at 25 meters/pixel scale resolution. There are numerous data gaps within the images, which may have created some uncertainty in the mosaic seams; therefore caution was used when analyzing orientations and sense of shear across the mosaic gaps. Strike-slip faults are noted with black numbers within white circles where the white arrows indicate the orientation of the strike-slip fault. The faults are: 1 = NW right-lateral, 2 = NW left-lateral, 3 = NE left-lateral, 4 = NE right-lateral. Illumination is from the east. Image numbers: s0374685413;26;27;39;52.

low resolution of the E6 images. Unclassified lineae are narrow, less than 500 meters wide, and generally extend for short (less than 50 km) distances in the E6 Conamara Chaos region. Higher resolution imaging of similar areas, such as the E4 region, suggests that these lineae are most likely troughs or double ridges (Ti, Trf, Rd).

2.3. Lenticulae

[17] Lenticulae (Figure 6) are defined as small (<20 km in diameter) subcircular to elliptical features, which are generally morphologically related [Pappalardo *et al.*, 1998a, 1999]. These features are generally spaced 15–25 km in the E4 and E6 regions [Spaun *et al.*, 2002]. Lenticulae consist of three types of features: domes (Ld, light gray), spots (Ls, dark gray), and micro-chaos pits (Lc, medium gray) [Head *et al.*, 1998a, 1998b; Pappalardo *et al.*, 1998a, 1999; Spaun *et al.*, 1999a, 1999b]. Domes are characterized by a broad, arched rise in topography on which preexisting structure is commonly preserved, implying that the surface has been bowed upward [Pappalardo, 2000]. Domes rise a few tens to hundreds of meters above the surrounding plains [Greeley *et*

al., 2000]. Central fractures have been observed to occur on domes and are noted in Figure 3 with a dashed line denoting the fracture upon the dome. We found six domes within the E6 area and none in the E4 area. The diameters of the E6 domes are from 3 to 13 km.

[18] Spots are topographically low areas of low albedo in which most of the background terrain has been destroyed, or possibly embayed and buried. Most spots exhibit a smooth texture, though some are hummocky and ridged. Spots have been called low-albedo smooth plains by other workers [Prockter *et al.*, 1999; Greeley *et al.*, 2000], though not all of the spots within our studied areas are smooth. Mapping of the embayment of predating structures in the “fishing hole” feature of the E4 region (upper right corner of Figure 3a, Figure 2) suggests a thickness of spot material on the order of tens of meters [Head *et al.*, 1998b]. There is also evidence of “kipukas”, isolated elements of ridged plains that appear to be completely embayed. The embayment of preexisting terrain suggests the emplacement of fluid cryovolcanic material and/or the disruption of previous structure possibly from near-surface melting caused by the

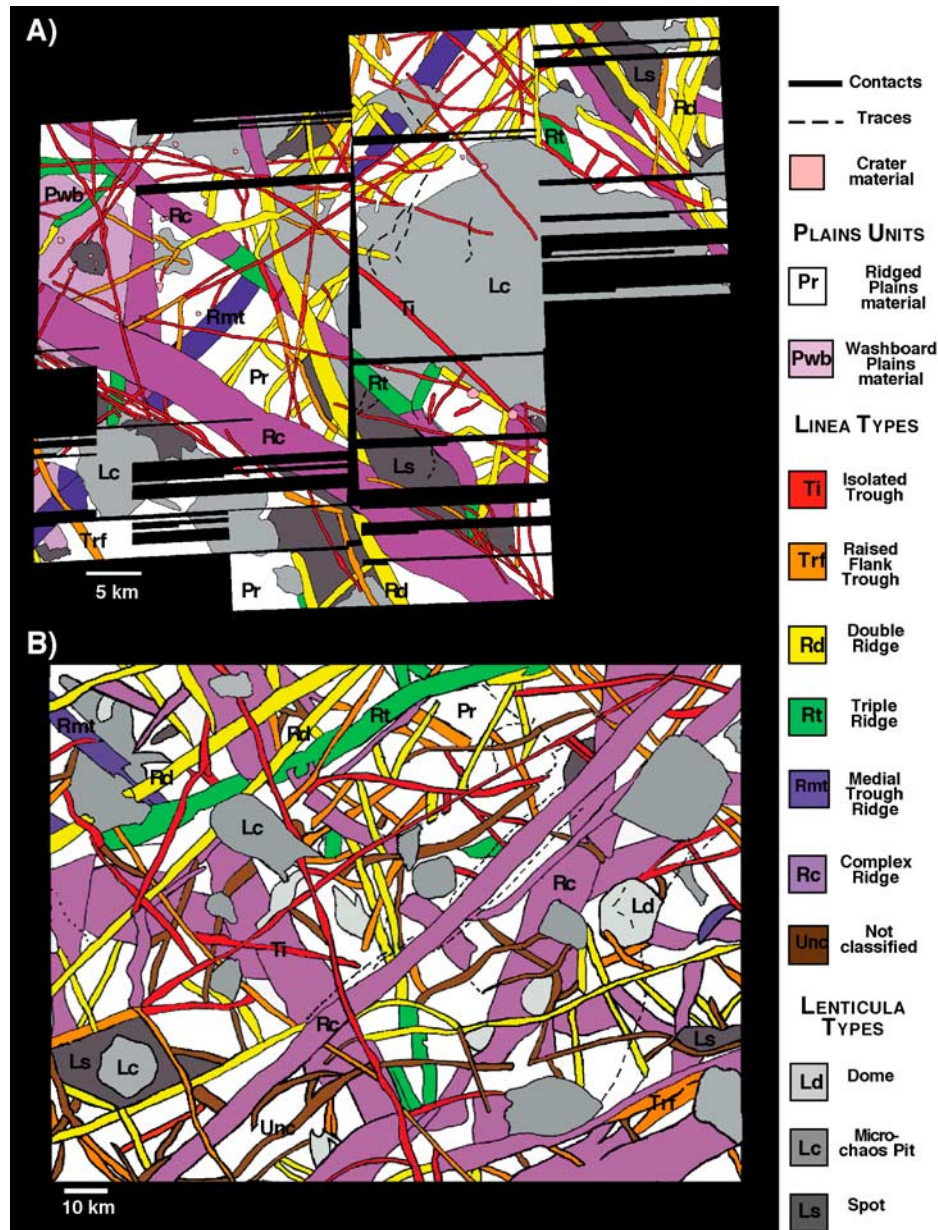


Figure 3. Geological maps showing recognized structures, units, and features. Adjacent legend applies to both maps. A) The E4 region, Figure 2. B) The E6 region, Figure 4.

presence of a thermal anomaly [Greeley *et al.*, 1998; Pappalardo *et al.*, 1998a, 1999; Head and Pappalardo, 1999]. Spots are fairly common within both mapped areas and can also be found surrounding other lenticulae. The diameters of these features are from 4 to 18 km in the mapped regions.

[19] Micro-chaos pits generally have an albedo that is lower than the ridged plains and they exhibit disruption of the ridged plains. Most micro-chaos lenticulae have rough textures and also contain polygons inferred to represent disrupted preexisting terrain. These polygons could be dislodged and dislocated fragments of background terrain that are frozen into the matrix, analogous to what is inferred in chaos regions [Carr *et al.*, 1998; Spaun *et al.*, 1998b,

1999b]. Micro-chaos lenticulae are common in both the E4 and E6 regions with diameters between 3 and 25 km.

[20] We infer that micro-chaos entails destruction of previous terrain units by fragmentation, disruption, tilting, and possibly foundering [Spaun *et al.*, 1998b, 1999b]. Some micro-chaos are associated with low-albedo smooth spots in moat-like surrounding areas where the low-albedo material is commonly bounded by topographically high lineae (Figure 6). Such embayment suggests an origin by heating from the subsurface and subsequent mobilization of surface material. In addition, alteration of the surface could be driven by rapid sublimation of ice [Fagents *et al.*, 2000], recrystallization of the icy surface [Head *et al.*, 1998b] and/or brine mobilization [Head and Pappalardo, 1999].

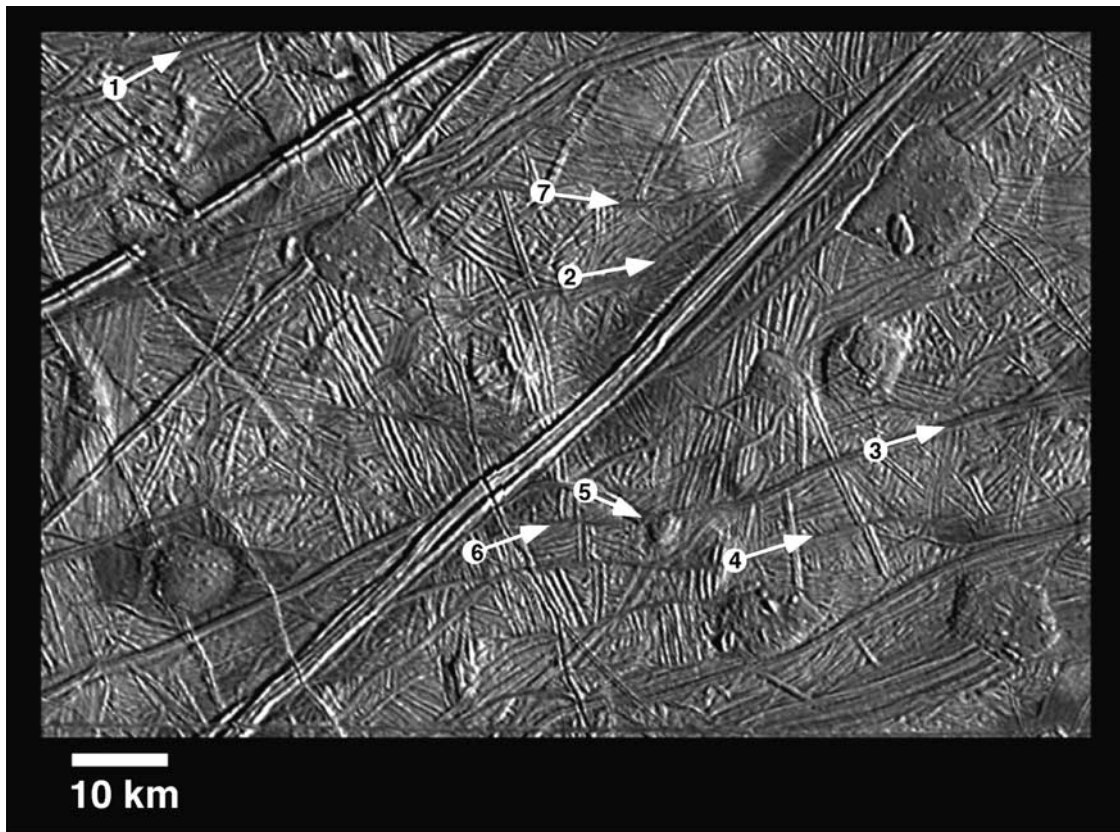


Figure 4. Image mosaic of the E6 region on Europa. Orthographic reprojection is centered at (10°N, 273°W) and the studied region is centered at (14°N, 271°W). Strike-slip faults are noted with black numbers within white circles where the white arrows indicate the orientation of the strike-slip fault. The faults are: 1 = NE left-lateral, 2 = NE right-lateral, 3 = NE right-lateral, 4 = NE left-lateral, 5 = NW left-lateral, 6 = E-W left-lateral, 7 = E-W right-lateral. Illumination is from the east; resolution is 180 meters/pixel. Image numbers: s0383713700;01;39.

[21] Various mechanisms of lenticula formation have been proposed, including diapirism and “melt-through” models. In the first case rising diapirs from a ductile layer underlying the ice surface cause upward surface flexure (as exhibited by domes), followed by localized heating, disruption, collapse, and extrusion (as seen in micro-chaos and spots) [Pappalardo *et al.*, 1998a; Pappalardo, 2000; Head *et al.*, 1998b]. In the second model a shallow ocean “melts through” a very thin overlying ice shell and creates spots and micro-chaos [Greenberg *et al.*, 1999], but does not account for the formation of domes.

[22] There is no apparent correlation between lenticula location or morphology, and linea location or morphology (Figure 3) in the studied regions. Therefore it is unlikely that lenticulae are created by mechanisms directly related to formation of lineae, such as extrusion along feeder dikes, where a linear arrangement of lenticulae would be expected. There are no specific lineament types which consistently bound or predate lenticulae.

[23] Using cross-cutting, overprinting, and embayment relationships, we are able to determine the relative stratigraphy of both the E4 and E6 regions. The stratigraphic analysis of the ridged plains, lineae, and lenticulae indicates that lenticulae are generally the youngest of the observed features in both regions (e.g., Figures 2, 4, and 6). Ridged

plains in both regions feature segmented linear features that are everywhere cross-cut and overprinted by individual lineae; thus ridged plains are determined to be the oldest observed geological unit. Individual lineae of a range of orientations are observed cross-cutting the ridged plains and washboard plains. Most lineae are cross-cut, dissected, and overprinted by lenticulae. Sharp scarps are observed at the intersections of lineae, ridged plains, and micro-chaos lenticulae, where lenticulae have disrupted the preexisting surface. Spots embay lineae, smoothing and/or darkening regions up to the flanks of lineae. Therefore lenticulae generally postdate individual lineae. There are some troughs, however, that cross-cut some lenticulae (Figure 6), suggesting that individual linea formation did not end with lenticula formation. A post-lenticula linea is easy to identify by the lack of disruption or dissection of the lineae as it crosses the hummocky matrix material within micro-chaos lenticulae. If lenticulae were generally older than lineae, we would expect to find numerous lineae with undisrupted or dissected flanks cutting the lenticulae. This is not observed; instead, there are only a few lenticulae-crossing lineae and most of these are troughs, not more complex lineae types. In the E6 Conamara Chaos region, there is evidence that lenticula and chaos formation occurred contemporaneously [Spaun *et al.*, 1998b]. We found no visible record of

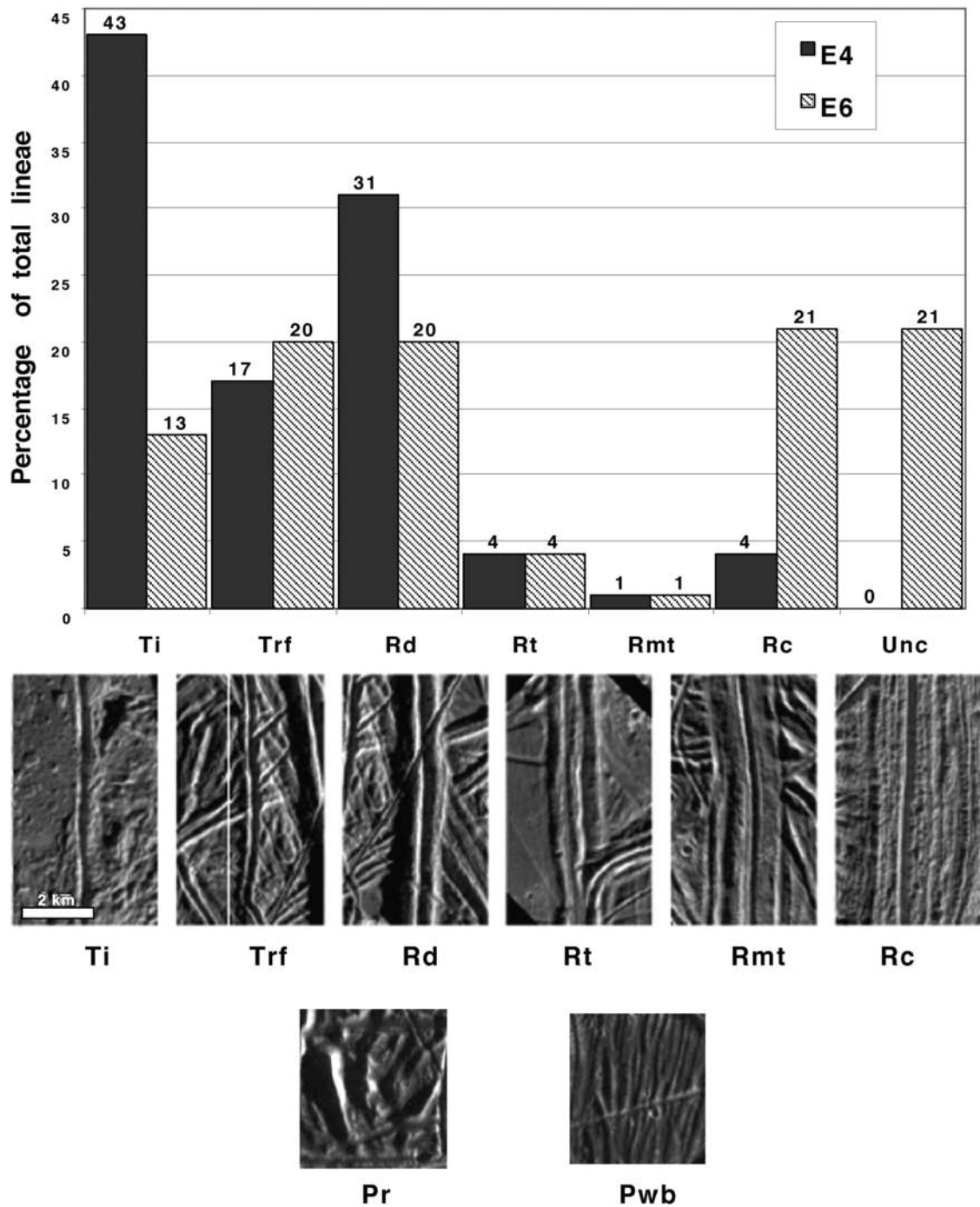


Figure 5. Linea and plains unit morphologies and distribution. Top: relative abundance of linea classes in the mapped areas. Bottom: examples of units, taken from the E4 high-resolution region. The classification scheme [Pappalardo *et al.*, 1998b; Head *et al.*, 1999] may also represent a possible evolutionary sequence for ridge formation, with initial stages at the left and later stages toward the right.

lenticula and chaos formation occurring in the E4 or E6 regions in earlier time periods (i.e., disruption in the ridged plains in early stratigraphic levels). On the basis of these relationships, we conclude that lenticulae in the E4 and E6 regions are relatively recent features. Similar stratigraphy has been inferred and documented elsewhere on Europa [e.g., Prockter *et al.*, 1999; Spaun *et al.*, 1999a, 1999b; Figueredo and Greeley, 2000; Kadel *et al.*, 2000] suggest-

ing that this stratigraphy may be characteristic of Europa [Greeley *et al.*, 2000].

3. Analysis of the E4 Region: Linea Abundance, Stratigraphy, and Orientation

[24] We will first explore the E4 region in detail with a focus on understanding the nature of lineae in the region.

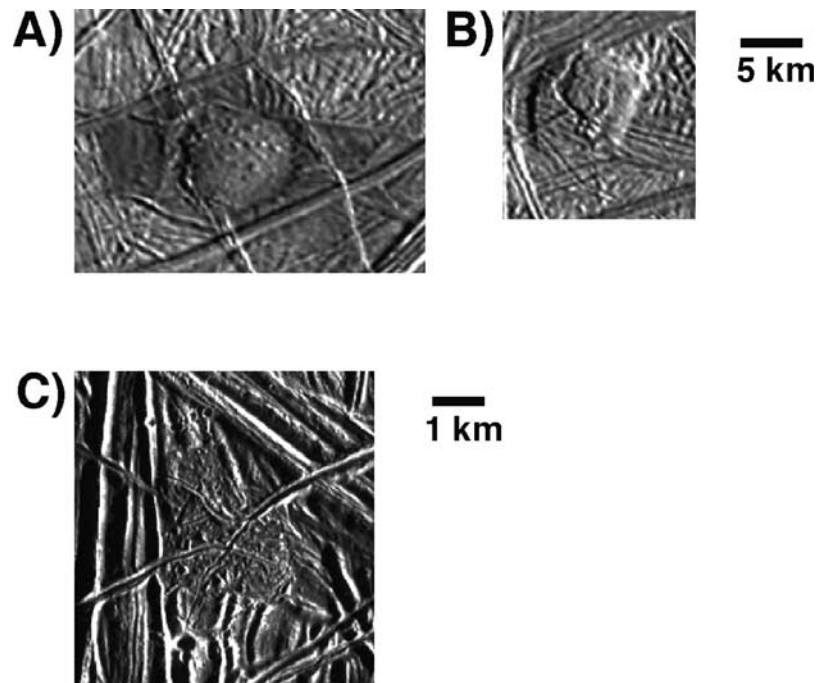
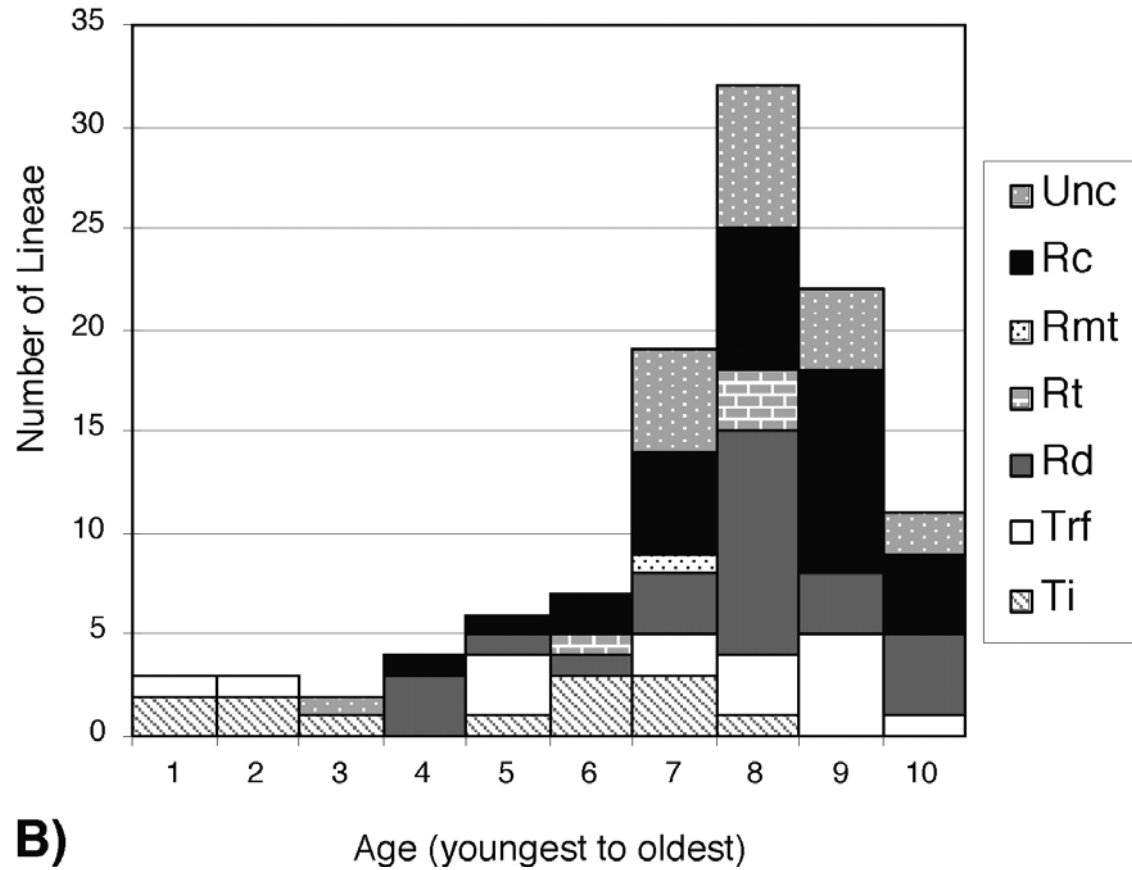
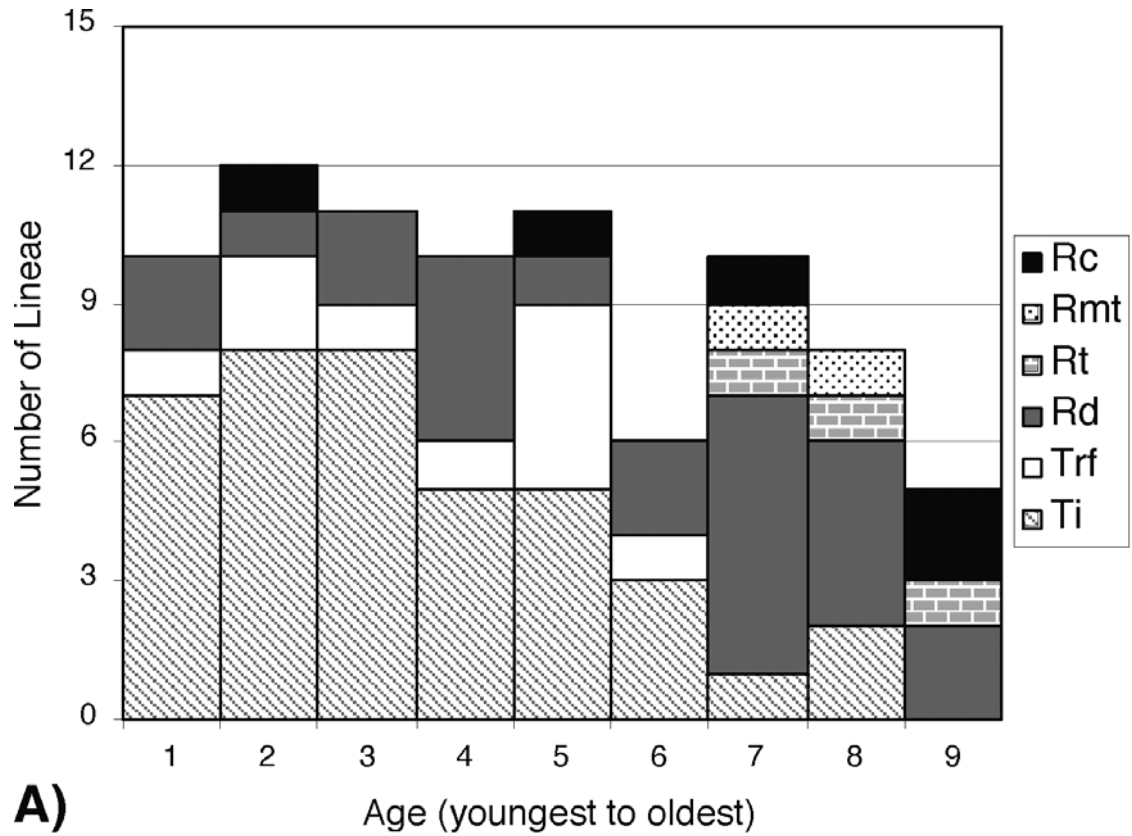


Figure 6. Lenticula from the E6 region (top) and E4 region (bottom). Scale bars are shown at right. A) A micro-chaos pit surrounded by low-albedo material. The moat-like low-albedo material appears to embay pre-existing terrain. It also has linear boundaries, which may be suggestive of barriers to fluid flow. B) A typical dome in that it upwarps without destroying the pre-existing terrain. The dome is unusual, however, in that it has a central fracture zone filled with disrupted material, which supports the hypothesis that domes may disrupt Europa's surface and evolve into pits [Pappalardo *et al.*, 1998a]. C) An example from the E4 high-resolution region of a pit which is cross-cut by several more recent lineae. This suggests that lineae formation continued beyond the period of lenticula formation. The micro-chaos is relatively very young though and this is determined by comparing the number of cross-cutting lineae to the number of lineae in the neighboring ridged plains.

We identified four lineae which show strike-slip displacements based on offset of preexisting structures; of these two are right-lateral and two are left-lateral. The relative abundances of lineae types, with an example of each class, are shown in Figure 5. Isolated troughs (Ti) occur in the greatest abundance, followed by double ridges (Rd). Raised-flank troughs (Trf) have a lesser abundance in the E4 region. The other ridge classes (Rt, Rmt, and Rc) are rare, together totaling 9% of the E4 region's lineae abundance. It is worthwhile to note that an individual lineae can vary in morphology along its length; in such an instance we mapped the lineae in segments, based on the morphology of each segment. For classification purposes, the lineae is identified by the morphology of the majority of its segments. Such variation in lineae suggests that lineae can evolve from simple types to more complicated morphologies either with time or possibly during emplacement due to differences in original conditions, such as variations in surface topography or local stresses.

[25] Our analysis also involves the relative abundance of lineae classes (Figure 5) compared to their stratigraphic ages (Figure 7). To obtain the lineae history of the area, we analyzed cross-cutting relationships among the different lineae types to see if there is any consistent change in morphology with age, and to test possible genetic and evolutionary relationships among the types. For example, Pappalardo *et al.* [1998b] and Greenberg *et al.* [1998] have each proposed evolutionary sequences in which isolated troughs could evolve into double ridges and then into more complex ridges. Like separating a mound of spaghetti, determination of relative stratigraphic ages for individual lineae is performed by analyzing how lineae overprint other features and lineae. These individual lineae are each assigned a stratigraphic age based on cross-cutting relationships, where lineae assigned a 1 are the most recent lineae and increasing numbers denote older generations (Figure 7). All lineae that are not crosscut by another lineae are therefore in the first generation. While these lineae may not have all

Figure 7. (opposite) The relative abundance of lineae morphologies as a function of relative age in the mapped regions. A) The E4 region: troughs (Ti and Trf) are more common in the recent history; double ridges (Rd) and complex ridges (Rc) are found throughout the stratigraphic levels; and triple ridges (Rt) and medial-trough ridges (Rmt) are restricted to the older levels. B) The E6 region: isolated troughs (Ti) are most abundant in the younger stages and taper off in abundance in the older stages; complex ridges (Rc) are most abundant in the older stages. The data from these regions suggest an evolutionary sequence of lineae morphologies with time.



formed at the same instant in time, they are stratigraphically contemporaneous and thus treated as one generation. Any lineae that are crosscut only by first generation lineae are thus second generation. A lineae crosscut by a second generation lineae is thus third generation and so on. Because this is a relative, and not absolute, chronology and the two regions are separated by over 50 degrees of longitude, we can only qualitatively compare the stratigraphy of lineae between the two regions. Using these methods of stratigraphic analysis, we discerned nine sequential stages of lineae formation within the E4 region (Figure 7a). It is important to note that the stratigraphy is determined by the cross-cutting relationships of ridges and troughs. These ridges and troughs originated as/from fractures that were acted upon by a geological process to make them into distinct troughs or ridges. Because the fractures may be acted upon later to make lineae, there is some uncertainty in inferring initial fracture stratigraphy from lineae stratigraphy. For example, two fractures can form contemporaneously though if one is of a more favorable orientation within the stress field, such that it will evolve into a lineae first and the second fracture next, we should observe one lineae cross-cutting the other where the two lineae meet. However, because most processes of ridge formation rely upon favorable stress conditions aligning with an initial fracture [e.g., *Greenberg et al.*, 1998; *Gaidos and Nimmo*, 2000] so that the two may evolve simultaneously, we thus infer a close relationship between the stratigraphy of fractures and the lineae they evolve into.

[26] In the E4 region, isolated troughs (Ti) are most abundant in the more recent stratigraphic levels though they are also found in the middle stages. However, isolated troughs are not found in the older generations of lineae in this region. Raised flank troughs (Trf) also occur only in the younger and middle stages, while triple ridges (Rt) and medial-trough ridges (Rmt) are restricted to the older generations of lineae. Double ridges can be found in all of the stratigraphic levels, though they have a greater abundance earlier in the region's history. The few complex ridges (Rc) in the E4 region are scattered throughout the stratigraphic record. The overall change in lineae style over time, from older complicated ridge types (Rd, Rt, and Rmt) to recent troughs (Ti and Trf), is consistent with the lineae evolutionary sequence of *Pappalardo et al.* [1998b] and *Greenberg et al.* [1998] in that younger, simple lineaments have presumably not had the opportunity to evolve into more complex forms. It is also possible that these lineae did not evolve with time and that more complex lineae types were favored early on in Europa's history; it is difficult to differentiate between these possibilities. If the lineae do not evolve with time and instead formed in their currently observed states, it is possible that the abundance of complex ridge types earlier in Europa's history and is related to the early formation of bands as well [*Prockter et al.*, 1999; *Figueredo and Greeley*, 2000]. However, a few complex ridge types have been observed in recent stratigraphic levels, contrary to the stratigraphy observed for bands and supporting the determination of complex ridges as distinct from bands.

[27] We also assess the orientations of the lineae within the E4 region (Figure 8a). Most of the lineae fall within two dominant trends: 30°–60° (note: 0° = North), NE, and

280°–340°, NW. Throughout the E4 region, E-W oriented lineae are extremely rare. Of the observed strike-slip faults, two faults (1RL = one right lateral, 1LL = one left lateral) are oriented NE while two faults (1RL, 1LL) are oriented NW.

[28] We also evaluated the orientations of lineae as a function of morphology (Figures 9a–9e). Isolated troughs are common in the dominant trends, though more are NW than NE. While very few lineae are oriented E-W, the majority of these lineae are middle-aged, isolated troughs (Ti). Raised flank troughs (Trf), double (Rd) ridges, and triple ridges (Rt) occurred in many orientations. No double ridges (Rd) or complex ridges (Rc) are oriented E-W, while several are found N-S. Complex ridges are predominantly of a NW orientation. In summary, the few lineae that are oriented E-W are isolated troughs (Ti) suggesting that lineae formed in this orientation may not have evolved into more complicated lineae types. The dominant trends are comprised of all classes of lineae, while some lineae types have a slight tendency toward NW or NE.

[29] We further examined lineae orientation as a function of age (Figure 10). Note that we were unable to determine the stratigraphy of all the measured lineae due to severe cross-cutting of older lineae (Figure 10j). Therefore the stratigraphic relationships identified below refer to the more recent recorded history (Figures 10a–10i). Lineae oriented in the NW direction are more common in the recent history, while NE oriented lineae are found throughout. N-S lineae are generally recent while E-W lineae occur in the middle stratigraphic levels. There is no evidence for a rotation, clockwise nor counterclockwise, of lineae formation with time. The implications of a systematic change in orientations over time will be further explored in section 5 and have been inferred in other regions by *Geissler et al.* [1998a, 1998b], *Prockter et al.* [1999], *Figueredo and Greeley* [2000], and *Kadel et al.* [2000].

4. Analysis of the E6 Region: Lineae Abundance, Stratigraphy, and Orientation

[30] The E6 Conamara region covers a larger area than the E4 region and contains a greater number of lineae. Figure 5 illustrates the relative abundances of each lineae class for each mapped region as percentages of the total number of lineae within that region. The relative abundance of lineae types in the E6 Conamara region (Figure 5) shows that medial trough ridges (Rmt) and triple ridges (Rt) are rarely observed in this area. This result is similar to that found in the E4 region, suggesting that these lineae types may be rare overall. Simple troughs (Ti) have two-thirds of the abundance of the other classes of lineae while the other lineae classes (Trf, Rd, Rc, and Unc) have approximately equal abundances of lineae. Also identified were seven strike-slip faults, where three are right-lateral and four are left-lateral; this resembles the equal distribution found in the E4 region and also that found by *Hoppa et al.* [1999a, 2000] in the larger Conamara region.

[31] We also analyzed the abundance of lineae types as a function of age (Figure 7b). Note that the stratigraphy within this region is not directly comparable to that of the E6 region; the regions are separated by over 50 degrees of longitude and there are few lineae to connect the regions.

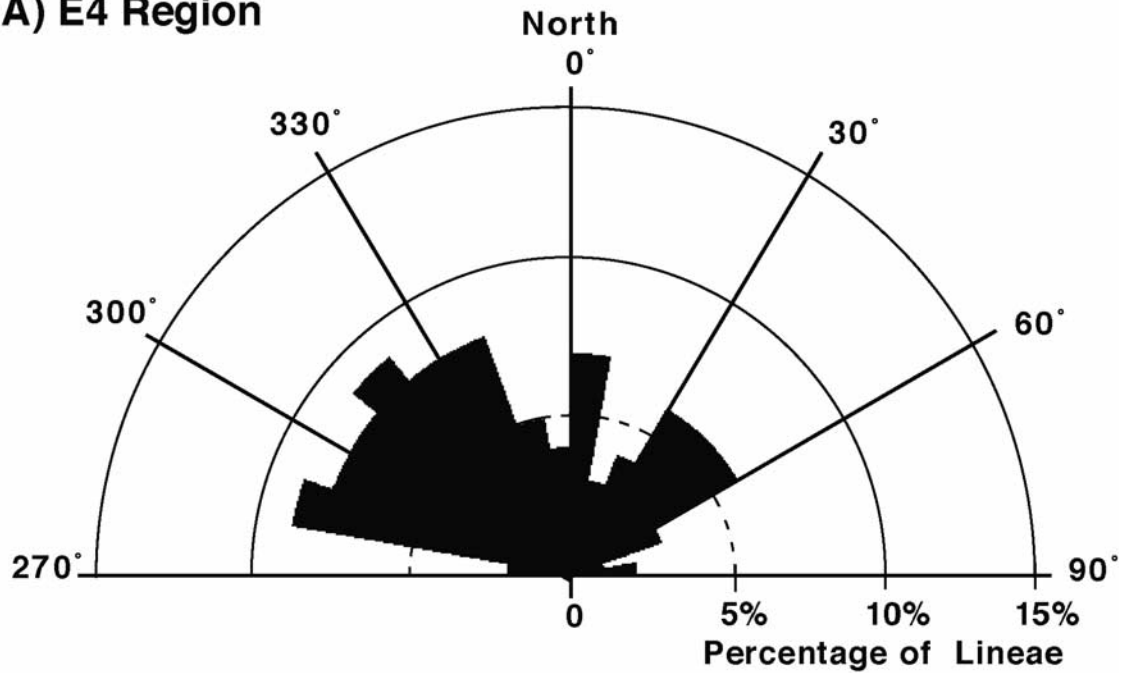
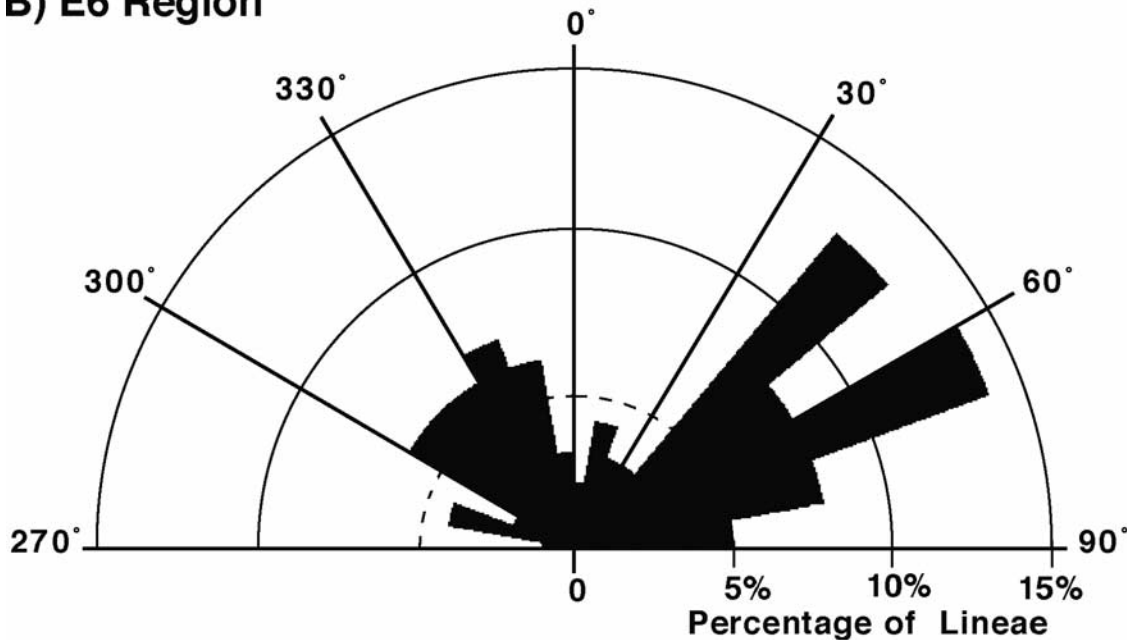
A) E4 Region**B) E6 Region**

Figure 8. The frequency distribution of lineae orientations in the mapped regions. The lineae were measured in 5 km segments and the data were normalized by dividing each bin by the total number of 5 km lineae segments within each mapped region. The rose diagrams thus depict the percentage of lineae of that orientation within each studied region. Percentage values above “5% of total lineae” are statistically significant and thus that value is depicted as a dashed arc contour; values below the 5% contour primarily concern the statistics of small numbers and therefore are less significant. This notation is consistent throughout the rose diagram figures. A) The E4 region. There are two major trends in the orientations of lineae within this region: 30°–60° (NE) and 280°–340° (NW). Few E-W lineae are observed, while many are clustered N-S. B) The E6 region. Two major trends are evident: 40°–70° (NE) and 300°–350° (NW). As in the E4 region, few lineae are oriented E-W.

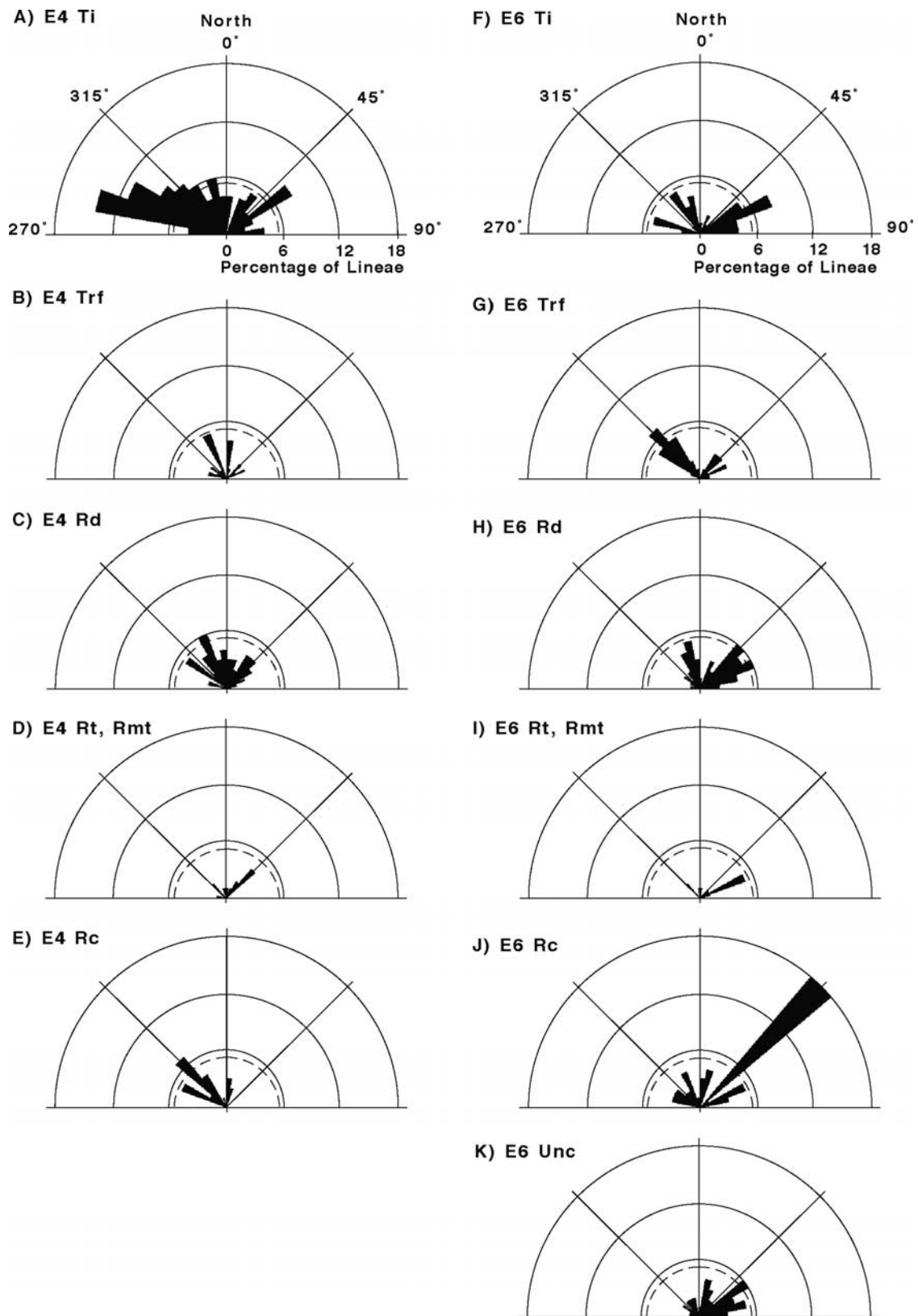
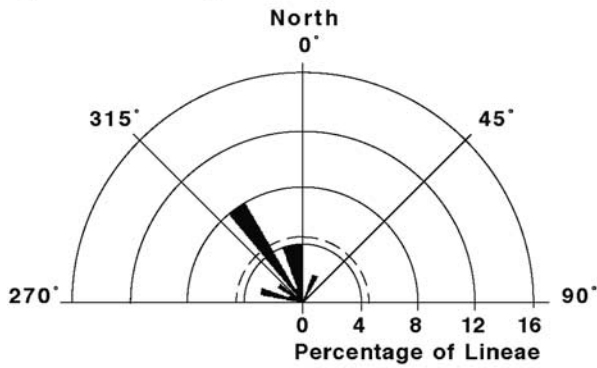
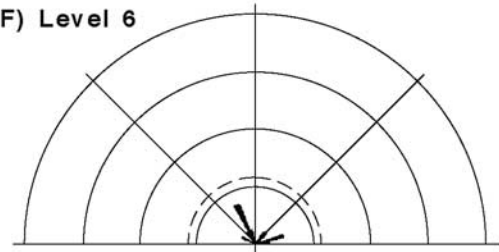


Figure 9. The frequency distribution of lineae orientations as a function of lineae morphology. A–E) Normalized data for the E4 region. F–K) Normalized data for the E6 region. The rose diagrams indicate that the majority of E-W lineae in both regions are isolated troughs (Ti), though the E6 region also has several E-W lineae that were unclassified (Unc).

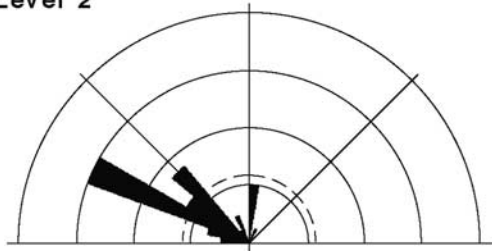
A) E4 Level 1 (youngest)



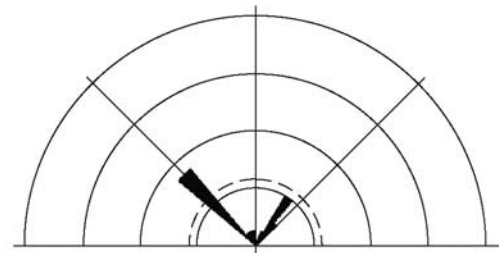
F) Level 6



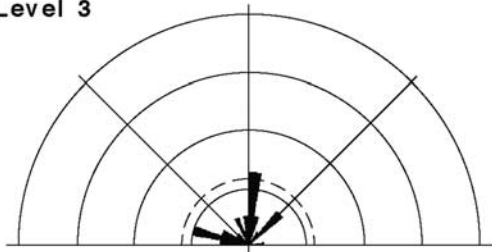
B) Level 2



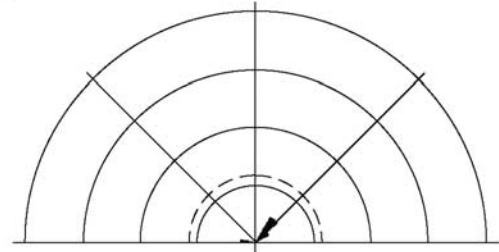
G) Level 7



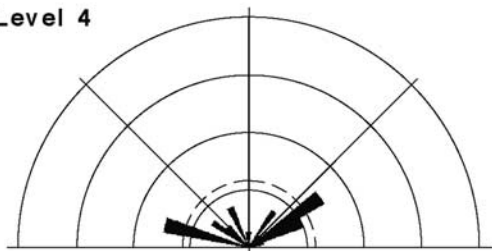
C) Level 3



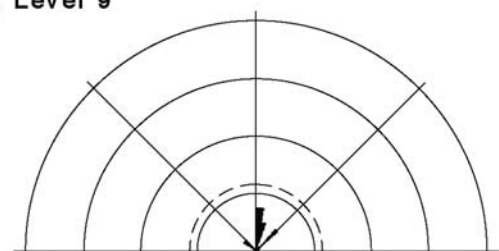
H) Level 8



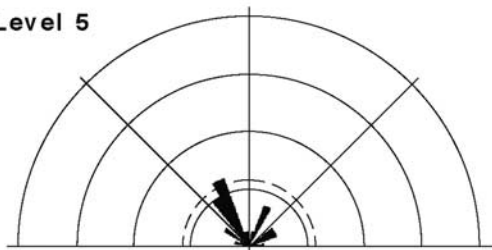
D) Level 4



I) Level 9



E) Level 5



J) Older levels

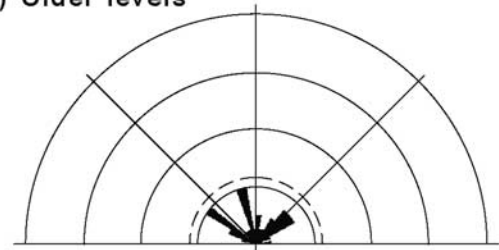


Figure 10. The frequency distribution of linea orientations as a function of stratigraphy for the E4 region. The rose diagrams are for the youngest through oldest (A–I) stratigraphic levels; older lineae that were not assigned a stratigraphic level are shown in J. Lineae oriented both NE and NW are found together within most of the stratigraphic levels. Most of the E–W lineae are within the middle stratigraphic levels. No clear rotation of lineae with time is observed.

The lineae stratigraphy of each region is a qualitative assessment of the history within that particular region. Isolated troughs are most abundant in the youngest and middle stages and are not found at all in the oldest stages; these results are similar to those of the E4 region. The apparent disappearance of isolated troughs in the older stratigraphic levels of this region could be due to their evolution into more complex forms, or might be due to the severe cross-cutting of lineae which would make them less recognizable by eliminating traces of narrow lineae as they become altered or blend into the ridged plains. Such apparent erasure of isolated troughs by cross-cutting could be enhanced by the lower resolution of the E6 images and explain the low number of Ti in the E6 region compared to the abundance of these troughs in the E4 high-resolution region. Of course, the E4 region also had a drop off of troughs (Ti and Trf) in the early stratigraphic record, suggesting that resolution may be a minor issue and the evolution of troughs into more complicated lineae types may be a more appropriate explanation of the observations. In the E6 region, raised flank troughs (Trf) are scattered throughout the stratigraphic record, while double ridges are intermediate to old in age. The majority of complex ridges are found in the older stages. The shifting of linea type abundances from young isolated troughs to older complex ridges is consistent with the evolutionary sequence of Pappalardo *et al.* [1998b] and Geissler *et al.* [1998a], and suggests that the simple linea forms have not had the opportunity to evolve into more complicated forms. Likewise, it could also be the case that these lineae did not evolve with time and complex lineae types were more likely to form early on in Europa's history.

[32] A thorough analysis of the orientations of the lineae in the E6 Conamara region was performed. We measured the trends of over 200 prominent mapped lineae (Figure 8b). Two dominant trends are found 40° – 70° , NE, and 300° – 350° , NW. The dominant NW and NE trends are narrower in range than the key NW and NE trends found within the E4 region, although the E6 regional trends are composed of more lineae. There is a dearth of lineae in the E-W orientation compared to the other trends; this is also true of the E4 area, suggesting that E-W lineae are typically rare in Europa's trailing equatorial region. Of the observed seven strike-slip faults, two faults (1RL, 1LL) are oriented E-W. Four faults (2RL, 2LL) are oriented NE, and one (1LL) is oriented NW.

[33] In general, different linea classes do not show exclusive orientations, but there are some tendencies in abundance with respect to orientation (Figures 9f–9k). For example, some lineae of each type can be found within both of the dominant trends (NW and NE). The majority of N-S lineae are double (Rd) and complex ridges (Rc). The majority of E-W oriented lineae are isolated troughs (Ti) and unclassified lineae (Unc), while there are few other linea types present with that orientation. While it may appear that

complex ridges (Rc) are dominantly oriented NE, this is only a artifact of the plots as that peak is comprised of just one long ridge.

[34] We also examined linea orientation as a function of age for the selected E6 region (Figure 11). The dominant NW and NE trends have occurred throughout most of the stratigraphically observable stages, as well as with all linea morphologies. This suggests that the stress regime responsible for NW and NE lineae formation must have been similar throughout the recorded history of this area. Furthermore, the NW and NE oriented lineae can generally be found within the same stratigraphic level, possibly suggesting contemporaneous formation. Kraft and Greeley [1997] found similar orientation patterns for the larger Conamara region. E-W lineae are found in the middle and oldest stages, except for one very young long narrow trough (Ti) located at the southern edge of the mapped region and oriented E-W. The middle-aged E-W lineae are arcuate and segments range between N-S and E-W orientations, suggesting that these lineae opened with N-S or E-W orientations and then propagated in the other direction in response to changing stress patterns [Hoppa *et al.*, 1999b]; thus the origin of these lineae is more complex. Short N-S and E-W lineae are found in the older stages indicating that the N-S and E-W lineae were created by conditions that did not persist throughout the history of this area, demonstrating that local stress fields have changed over time. Further change is demonstrated by the youngest stratigraphic levels, which have both NE and NW lineae in the same levels with dominance in trend swinging back and forth. While recent work by Kattenhorn [2000] has inferred two complete rotations of lineae have occurred in a neighboring region at (15° N, 273° W), we find no convincing evidence of rotation of lineae with time in the E6 region.

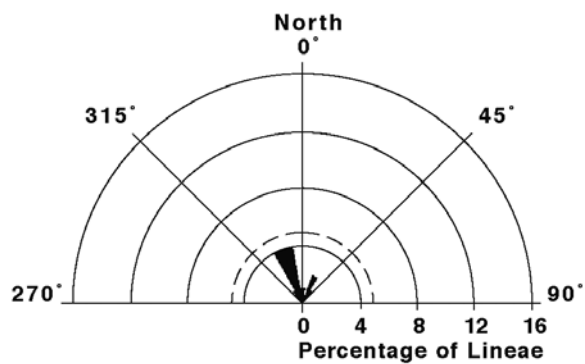
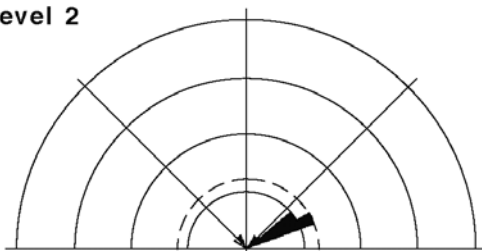
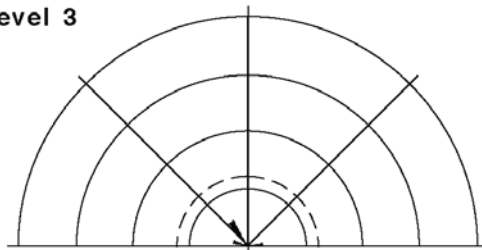
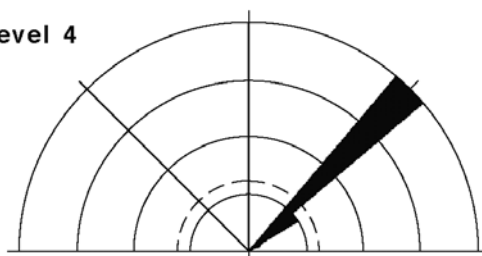
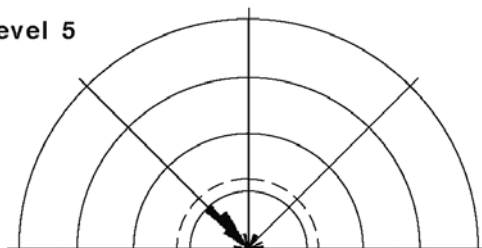
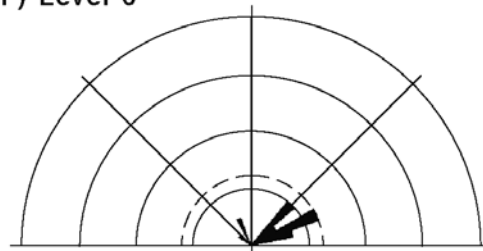
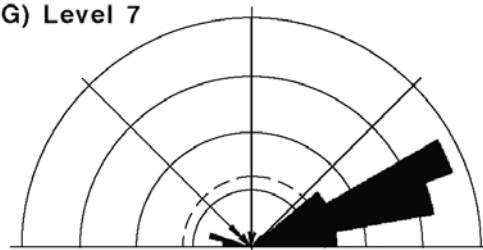
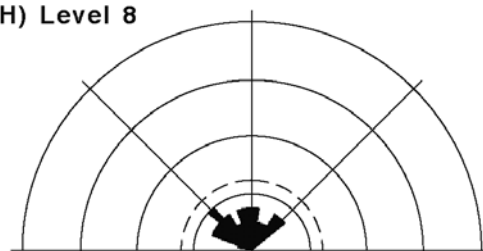
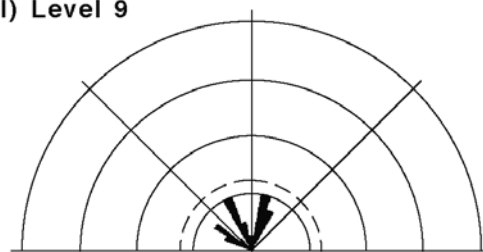
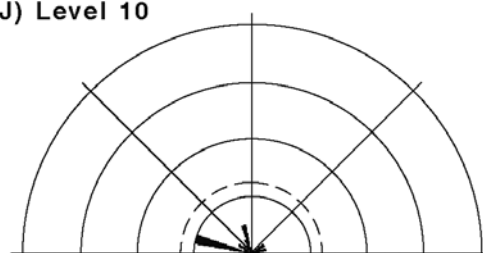
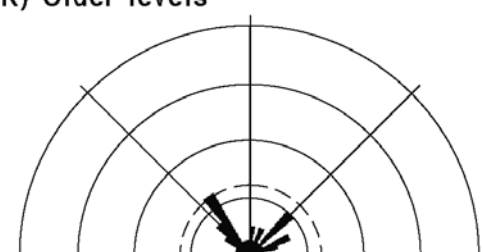
5. Synthesis

5.1. Global Stress Models

[35] The analysis of the lineae within the E4 (5° N, 327° W) and E6 (14° N, 271° W) regions has implications for Europa's global stress fields and tectonic history, as well as the mechanisms of linea formation. Both of the studied areas are located within the trailing hemisphere of Europa in the equatorial region (Figure 1). Previous workers have had difficulty in explaining the orientations and intersection angles of lineae within the equatorial leading and trailing quadrants if lineae formed as tension fractures [e.g., Leith and McKinnon, 1996; Greenberg *et al.*, 1998]. Therefore we have considered the predictions of several tectonic stress models (Figures 12 and 13) for comparison with the new data.

[36] First, stresses from global despinning [Melosh, 1977] were reviewed in assessing the orientational trends. The global despinning theory suggests that a body with an initially faster rotation rate will lose its equatorial bulge,

Figure 11. (opposite) The frequency distribution of linea orientations as a function of stratigraphy for the E6 region. The rose diagrams are for the youngest through oldest (A–J) stratigraphic levels; older lineae that were not assigned a stratigraphic level are shown in K. Lineae oriented both NE and NW are found together within many of the stratigraphic levels, though there is a tendency in levels 1–6 for orientation to swing back and forth, as also found by Kraft and Greeley [1997]. Most E-W lineae are within the older stratigraphic levels. No clear rotation of lineae with time is observed.

A) E6 Level 1 (youngest)**B) Level 2****C) Level 3****D) Level 4****E) Level 5****F) Level 6****G) Level 7****H) Level 8****I) Level 9****J) Level 10****K) Older levels**

Global Despinning and Orbital Recession Models

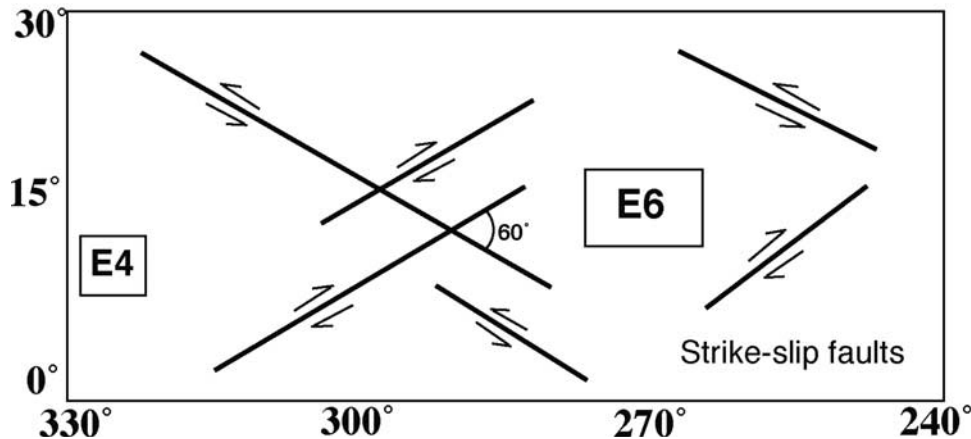


Figure 12. Predictions of global despinning [Melosh, 1977] and orbital recession [Melosh, 1980] models as applied to Europa. The locations of the E4 and E6 regions are noted on the diagrams and the boxes are approximately to scale. In the equatorial region, both models predict NE and NW oriented strike-slip faults, with intersection angles of $\sim 60^\circ$. Lineae in the E4 and E6 regions are observed to be predominantly NE and NW, yet in contrast to the predictions here the observed lineae are equally left and right lateral in strike-slip independent of orientation.

thus oblateness, as its spin slows and it reaches a synchronous lock with the parent body. The equatorial regions will thus undergo horizontal stresses that are both compressional and extensional, inducing predictable fracture patterns [Melosh, 1977]. While bodies with thicker elastic lithospheres will be dominated in the equatorial regions by thrust faulting, a thinner-shelled body like Europa should be dominated near the equator by conjugate sets of strike-slip faults [Melosh, 1977]. Helfenstein and Parmentier [1980] suggest that despinning-induced faults on Europa would intersect with angles between 30° and 90° . The model predicts that NE-oriented faults will be right-lateral while NW-oriented faults are left-lateral (Figure 12). This range is consistent with the NW and NE trends we have found within both the E4 and E6 regions (Figure 8). Conjugate shear faulting is also consistent with NE and NW lineae occurring closely in the stratigraphic record. However, the

observed correlation of fault orientation with sense of shear (listed by “number of faults - orientation - sense of shear”: 3-NE-RL, 1-NW-RL, 1-EW-RL; 3-NE-LL, 2-NW-LL, 1-EW-LL) does not match the predictions (all-NE-RL; all-NW-LL) put forth in the global despinning model. It is possible the observed sense of shear did not originate with the formation of the lineae and that diurnal ideas later acted upon the lineae to create the observed strike-slip [Hoppa *et al.*, 1999a, 1999b, 2000]. The greatest challenge to the despinning model is Europa’s extremely young surface age, nominally ~ 50 Ma [Zahnle, 2001]. Global despinning should have occurred extremely early in Europa’s history. The young surface age implies a resurfacing rate suggesting that any evidence of global despinning should no longer be recognizable.

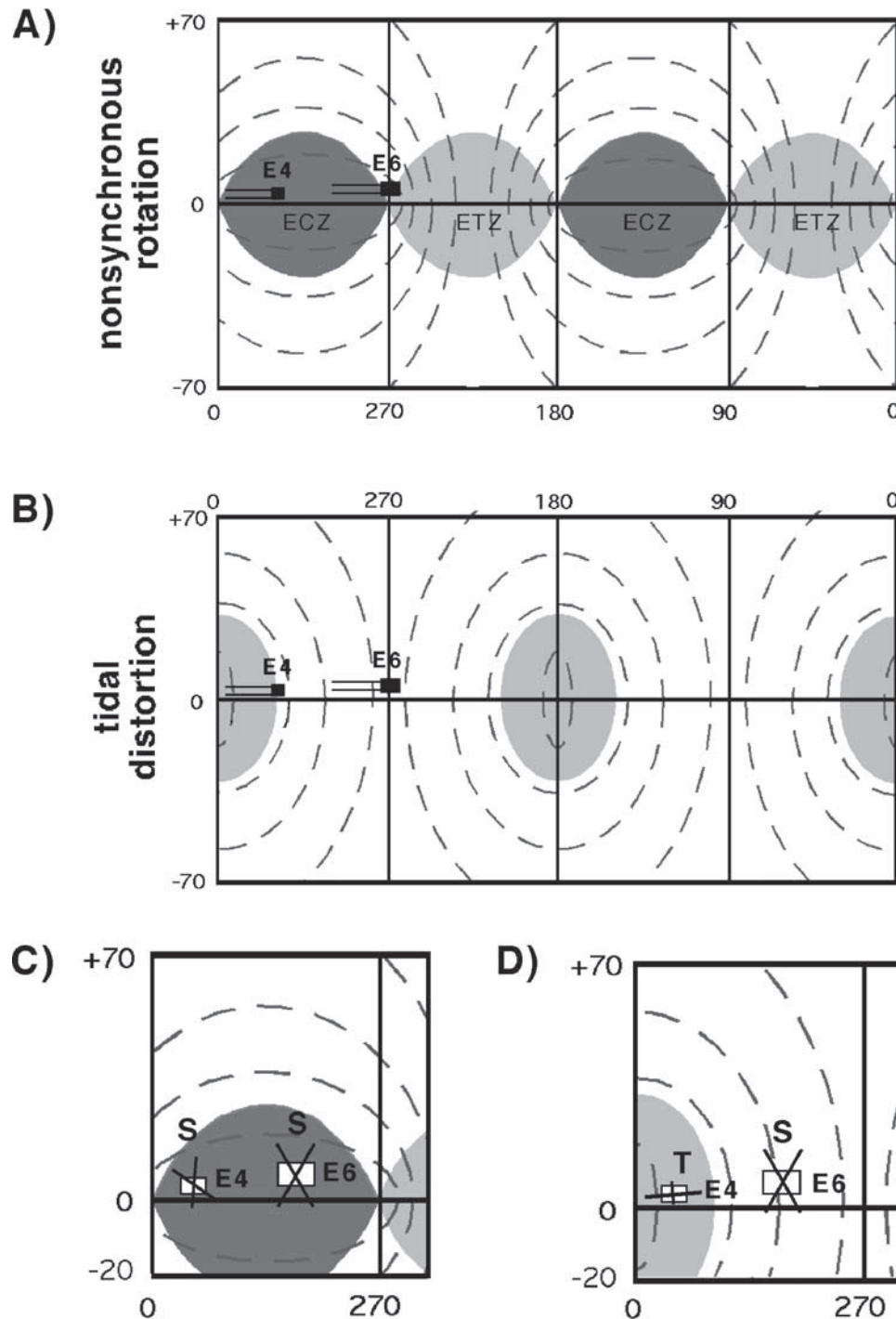
[37] Another theory evaluated was that of orbital recession [Melosh, 1980]. It suggests that a body with an orbital

Figure 13. (opposite) Diagrams of the global stresses produced by nonsynchronous rotation and tidal distortion [after McEwen, 1986] (used with permission from *Nature* (<http://www.nature.com>)) shown with predictions for the E4 and E6 regions. Dashed lines represent tensile stress trajectories. Light gray shaded ovals are regions where both horizontal principal stresses are tensile (— —) and dark gray ovals are regions where both principal stresses are compressive (+ +). Locations of the E4 and E6 regions in A and B are noted by black boxes. It has been suggested that the major European lineae formed an average of $\sim 30^\circ$ W of their current locations; therefore, the double black lines adjacent to the boxes indicate the past locations of the E4 and E6 regions, back as far as 30° in rotation. A) The global stresses due to nonsynchronous rotation create equatorial zones where both horizontal principal stresses are either compressional (Equatorial Compressional Zones, + +, denoted ECZ) or tensile (Equatorial Tensile Zone, — —, denoted ETZ). B) The global stresses due to diurnal tides at perijove; at apojove the signs of the principal stress directions are reversed (the tensile region becomes a compressional region and the dashed stress trajectories would become compressional). C) Predictions of structural orientations from nonsynchronous rotational and (D) diurnal tidal stress for the E4 and E6 regions shifted 30° W of their current locations (white boxes). Nonsynchronous rotational stresses are generally many times stronger than diurnal tides, thus having a stronger effect on the studied regions (see Figure 14). Predicted orientations of shear faults (S) and tension cracks (T) are shown. At apojove, the signs of the diurnal principal stresses reverse and thus the S and T features of diagram (D) will switch; thus, near apojove the E4 region could experience shear faulting and the E6 region tension cracking.

period longer than its parent body will recede from the primary and its tidal bulge will relax with time, creating the greatest stress difference at the limbs (the leading and trailing quadrants) [Melosh, 1980]. The combination of E-W compression and N-S extension would drive strike-slip faulting similar to the global despinning model (Figure 12). This model has the same difficulties as the global despinning theory: the observed strike-slips do not match the predictions and Europa has an extremely young surface age, while orbital recession should have occurred early in Europa's history. Interestingly, when the Melosh [1980] theory was

applied directly to Europa by Helfenstein and Parmentier [1983] they noted that the shear strength of polycrystalline ice is ~ 10 times greater than its tensile strength and thus concluded that the lithosphere should fail more readily in tension than in shear. Since then most lineae studies have thus also concluded that lineae are more likely to be tension fractures [e.g., Helfenstein and Parmentier, 1985; Greenberg *et al.*, 1998].

[38] Subsequent modeling considered nonsynchronous rotation effects on Europa [Greenberg and Weidenschilling, 1984; Helfenstein and Parmentier, 1985; McEwen, 1986;



Greenberg *et al.*, 1998]. This process could occur on Europa if the outer shell is decoupled from the interior and rotates slightly faster than the satellite's tidally locked interior. Diurnal stressing may have also affected the E4 and E6 regions. Europa orbits Jupiter every 3.55 days, and during that period its orbital eccentricity induces tidal flexing of the satellite. As a result, the tidal bulge increases as Europa approaches perijove and decreases as Europa approaches apojoive. Surface stresses due to nonsynchronous rotation would be induced by the progressive angular displacement of the tidal axis and thus the relocation of a tidal bulge [Helfenstein and Parmentier, 1985; McEwen, 1986]. Nonsynchronous rotation would cause a given region of Europa's surface to move eastward over time with respect to the tidal axes. As a result, the orientations of stresses, and thus lineae, are expected to rotate with time: clockwise in the northern hemisphere and counterclockwise in the southern [Geissler *et al.*, 1998a]. Predictions for the near-equatorial regions are different and we examine them in detail.

[39] The magnitudes of nonsynchronous rotational stresses are greater than that of diurnal tides for $>1/8^\circ$ of nonsynchronous rotation and thus we consider nonsynchronous rotation first and then consider diurnal tides (Figure 13). Stresses due to an infinitesimal nonsynchronous rotation indicate that the E6 region should presently undergo extremely weak tensile stresses oriented nearly N-S, while the E4 region should be subject to both axes as compressional principal stresses (Figure 13a) [see also Greenberg *et al.*, 1998]. However, if nonsynchronous rotation has occurred, it is likely that the observed lineae formed at longitudes somewhat westward of their current locations. Previous studies [McEwen, 1986; Leith and McKinnon, 1996; Geissler *et al.*, 1998b] have suggested that Europa's prominent lineae record an average of 30° of eastward surface migration due to nonsynchronous rotation; therefore, Figure 13c illustrates the locations of the study regions shifted west $\sim 30^\circ$. For this configuration, the E6 region is centered in an ovoidally shaped equatorial zone in which both principal horizontal stresses are compressional (henceforth the "equatorial compressional zone" or ECZ). The E4 region has been located in the ECZ over the past several tens of degrees of nonsynchronous rotation (Figures 13a and 13c). If lineae form only as tension cracks, no lineae are expected to form within the ECZ. Greater amounts of nonsynchronous rotation have been suggested [Figueroa and Greeley, 2000; Kattenhorn, 2000], such that lineae formed outside of the ECZ and within the ETZ. Strong tensile stresses near the equator due to nonsynchronous rotation are predicted to be oriented N-S, and thus consistently should form only E-W lineae (Figure 13a). To the contrary, analysis of the E4 and E6 regions indicate that E-W lineae are the most rare lineae within both regions. No rotation of lineae orientations is predicted, or observed, for near-equatorial regions. To summarize, no tension cracks should form within the ECZ and only E-W tension cracks should form within the ETZ. Simply rotating the shell by any amount should not yield the observed NE and NW lineae as tension cracks without the addition of another model component, such as that owing to polar wander [e.g., Ojakangas and Stevenson, 1989]. However, polar wander is not indicated by studies of

Europa's global-scale lineae [Leith and McKinnon, 1996; Greenberg *et al.*, 1998]. Moreover, polar wander alone could not explain the formation of NE and NW lineae within similar stratigraphic levels.

[40] Our evaluation of the existing tectonic models compels us to consider the possibility that lineae in the studied regions formed as conjugate shear faults within Europa's ECZ. Europa's surface in an ECZ is subject to strong N-S and moderate E-W compressional stresses. Shear faults oriented NE and NW, with intersection angles $\sim 60^\circ$ to each other, are predicted to form if shear failure occurs (Figure 13c). While shear failure was previously rejected because of laboratory measurements based on polycrystalline ice [Helfenstein and Parmentier, 1983], it has since been suggested that Europa's surface may also be highly fractured and contain numerous impurities (see Pappalardo *et al.* [1999] for a review). Concentrations of impurities and prefractured ice may potentially allow shear failure to occur more readily within ECZs. Furthermore, increased image resolution obtained with the Galileo mission has lead to more detailed analysis of lineae orientations; these observations are not consistent with predictions for tension cracks in the near-equatorial regions. Therefore we consider the possibility of nonsynchronous rotational stresses generating shear failure in forming lineae within the near-equatorial trailing regions.

[41] It is likely that diurnal tides may have also acted on the studied regions, acting as an additive or subtractive force to nonsynchronous rotational stresses. Figure 13b illustrates the predictions for the stress patterns due to tidal distortion in the studied regions. For a maximum tidal bulge (near perijove), strong N-S and weaker E-W tensile stresses are predicted for the E4 region, and N-S compression and negligible E-W stress is predicted for the E6 region. Diurnal tide models predict that the maximum differential stress (the difference between normal and tangential components of stress) across Europa's surface [Helfenstein and Parmentier, 1983] should occur near the E6 region over the last 30° of nonsynchronous rotation. Adding in compressional principal stresses from nonsynchronous rotation will create a maximum N-S compressional stress and a weak E-W compressional stress (Figure 14), thus further increasing the differential stress between normal and tangential components. In the E6 region, conjugate shear faults are expected to form oriented both NE right-lateral and NW left-lateral (Figures 13c, 13d, and 14) while structural trends are rotated only slightly counterclockwise from this in the E4 region (Figures 13c and 13d). Figure 14 is the strain ellipse predicted for 30° of nonsynchronous rotational stresses in the equatorial trailing region combined with diurnal stresses from a maximum tidal bulge near perijove.

[42] For a decreasing tidal bulge, compressional and tensile diurnal tidal stresses reverse. For larger degrees of nonsynchronous rotation, $>1/8^\circ$, N-S tensile stresses and weak E-W compressional stresses due to diurnal tides will combine with compressional principal stresses from nonsynchronous rotation to create an overall moderate N-S compressive stress and an E-W compressive stress; thus a decreasing tidal bulge also results in a maximum differential stress in the studied regions generating NE right-lateral faults and NW left-lateral faults. For small amounts of nonsynchronous rotation, $\sim 1/8^\circ$ or less, the magnitude of

Perijove

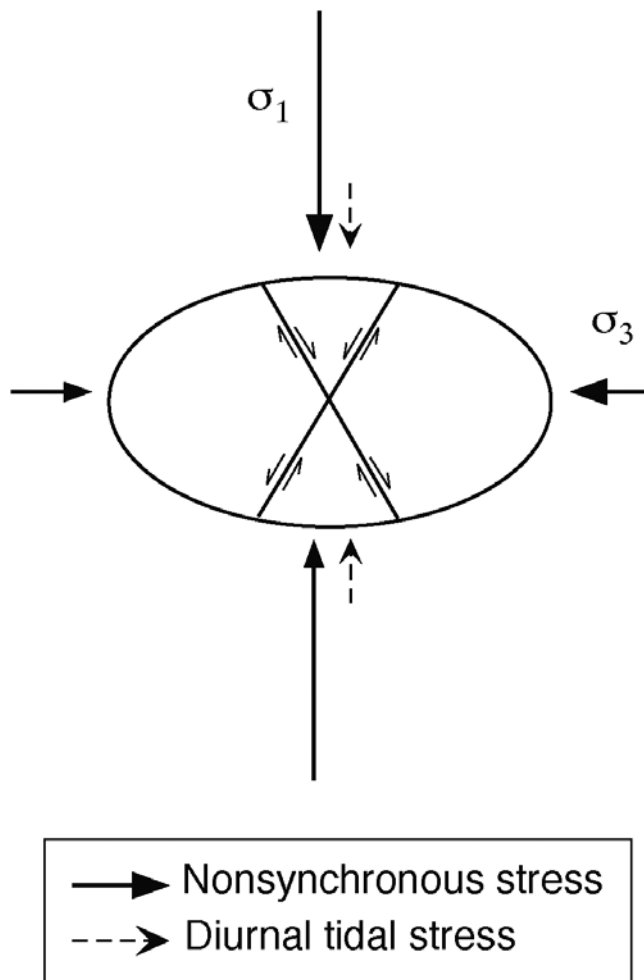


Figure 14. Strain ellipse depicting the stresses predicted near perijove 30°W of the current E6 location. During perijove, when the tidal bulge is near maximum, the diurnal tidal stresses in this location are compressional and oriented N-S; near apojove, the diurnal stresses are of the same magnitude but opposite in sign. The stress vectors are shown to scale based on the data presented by *Greenberg et al.* [1998] for $1/2^\circ$ of nonsynchronous rotation. Note that for smaller degrees of nonsynchronous rotation the diurnal tides are relatively stronger; for $\sim 1/8^\circ$ or less of nonsynchronous rotation the strain ellipse effectively rotates 90° from that shown at apojove. For larger degrees of nonsynchronous rotation ($>1/2^\circ$) the diurnal tidal stresses become negligible. Generally, the strong compressional stresses from nonsynchronous rotation within the ECZ dominate and shear failure is predicted.

diurnal tides may overcome nonsynchronous rotational stresses, generating a strong E-W compressive stress approaching apojove. These stresses would reverse the strain ellipse in Figure 14 and generate NE left-lateral faults and NW right-lateral faults. The cycling between increasing and decreasing tidal bulges owing to orbital eccentricity, combined with modest angular rotation of stress due to the

eastward movement of the European shell from nonsynchronous rotation, could account for the angular spread in generally NE- and NW-trending lineae and the equal distribution of right- and left-lateral faults observed within the E4 and E6 regions.

[43] We can consider the relationships between lineae orientation and age to further assess the shear failure hypothesis. The rarity of E-W oriented lineae in the E6 region is consistent with formation of most of its lineae by a mechanism other than tension cracking; we suggest that shear failure generated the NE and NW lineae. In the E6 region, the stratigraphy of E-W lineae, which are inferred to have formed outside the ECZ, supports this interpretation: the E-W lineae generally occur in the older generations and presumably would have formed before the E6 region entered the ECZ. There are a few middle-aged isolated troughs but these are arcuate, potentially cycloidal, and so are more likely related to rapid formation controlled by diurnal stresses [*Hoppa et al.*, 1999b], where nonsynchronous rotation stresses are relatively small on short time-scales. One E-W isolated trough, which is the youngest linea in the mapped region, could have formed when the region emerged from the ECZ and achieved its present position. The E4 region has proportionately more, yet shorter, E-W lineae than the E6 region. This is expected, as it is predicted to have spent more of its history outside the ECZ while only relatively recently entering this zone. The E4 and E6 regions have been located at positions of minimal tensile stresses which impedes tension cracking, such that over the past several tens of degrees of nonsynchronous rotation, any failure of the ice in these regions would have to be in shear (as conjugate shear faults) or in compression (as folds or thrusts).

[44] The other location on Europa that has most recently emerged from an ECZ, and where the differential stress is a maximum, is the near equatorial region of the leading quadrant. Analysis of the leading quadrant therefore provides a good test for the conjugate shear fault hypothesis explored above. Recent work by *Figueredo and Greeley* [2000] focused on mapping of images obtained by Galileo during its 15th Jovian orbit (orbit E15). We are most interested in the section of the E15 image mosaic from 2°S to 30°N and from 72°W to 85°W , as this region is antipodal to the E6 region. The orientations of lineae within the E15 region are strikingly similar to those observed within the E6 region: most of the lineae are oriented NE and NW, and E-W are rare and those present occur early in the stratigraphic column. *Figueredo and Greeley* [2000] suggest that these lineae have formed as tension cracks which have rotated in orientation through time, consistent with a model combining a complete 360° nonsynchronous rotation and cyclic diurnal tides. However, such an interpretation inappropriately requires tension cracks to form in ECZs where no tensile stress exists. Furthermore, only E-W tension cracks should form within ETZs. The paucity of predicted E-W lineae near the equator is unexplained. We can reconcile the observations in the E15 region with those of the E6 region if Europa has undergone $<90^\circ$ of nonsynchronous rotation, which brought the leading and trailing quadrant equatorial regions into zones of minimal tensile stresses and maximum differential stresses. These unique locations inhibited E-W tensile fracturing and

instead allowed shear failure to occur, forming the observed predominant trends of NE and NW lineae.

[45] The formation of lineae in shear has important implications for ridge formation models. Models which rely solely on tension to create all fractures and ridges [e.g., *Greenberg et al.*, 1998] are challenged. Many models work equally well with extensional and shear failure fracturing. Ridge formation models that take advantage of shear heating to aid in linear diapirism perhaps in combination with partial melting, [*Head et al.*, 1999; *Gaidos and Nimmo*, 2000], are favored.

5.2. Geological History

[46] Geological mapping of these regional and high-resolution image mosaics show that these areas of Europa's surface are generally composed of ridges, troughs, lenticulae, and highly segmented ridged plains; larger chaos regions are present nearby [e.g., *Greeley et al.*, 2000; *Spaun et al.*, 1998a, 1998b]. Geological mapping and stratigraphic analysis show the following sequence of events in these areas, from oldest to youngest: 1) formation of ridged plains, 2) formation of individual lineae (ridges and troughs), 3) widespread occurrence of lenticulae, 4) continued formation of troughs and double ridges. Lineae of a range of specific morphologies, in a possible sequence of evolution, have formed through tensile and shear failure throughout the observable stratigraphic sequence in these areas.

[47] Throughout the high-resolution E4 region, we infer three basic stages in the geological history, only varying from the E6 region in orientation of lineae: 1) Formation of ridged plains and washboard plains, a subset of ridged plains. 2) Formation of a range of individual cross-cutting troughs and ridges, dominantly oriented NE and NW, and 3) formation of lenticulae and continued linea formation, with the youngest lineae tending to be isolated troughs. We found no evidence for development of lenticula features earlier in the stratigraphic sequence, such as contemporaneous with the ridged plains.

[48] In the E6 region, during the period postdating ridged plains formation, individual ridges formed in a range of orientations. The next period is typified by lineae oriented predominantly in the NW and NE directions, inferred to have formed conjugate as shear faults; the morphology of the lineae formed during this period was characterized by fewer complex ridges and more abundant double ridges and troughs. Subsequent to this, lenticulae (micro-chaos, spots and domes) began to form with continued individual lineae formation.

[49] The formation of lenticulae, generally the youngest features, has been interpreted as an endogenic process [*Greeley et al.*, 1998, 2000; *Pappalardo et al.*, 1998a]. Our mapping supports this interpretation; the range of morphologies of lenticulae (see section 2.3), their size and spacing are consistent with an interpretation of their formation by rising diapirs and associated cryomagmatism [*Pappalardo et al.*, 1998a; *Spaun et al.*, 1998a, 1998b, 1999a, 1999b]. Similar stratigraphy to that interpreted here has been inferred in other areas of mottled terrain [e.g., *Prockter et al.*, 1999; *Figueroa and Greeley*, 2000; *Kadel et al.*, 2000], in contrast to the findings of *Riley et al.* [2000]. We infer that regional-scale processes have acted on bright plains to create the

lenticulae and chaos features that disrupt the surface, converting Europa's plains into mottled terrain.

6. Conclusions

[50] Previous global stress models have been unable to explain the orientations and intersection angles of lineae at the near-equatorial regions of Europa's leading and trailing regions [e.g., *Leith and McKinnon*, 1996; *Greenberg et al.*, 1998]. The mapped E4 and E6 regions are within the trailing hemisphere and were studied in detail. The dominant orientations of observed lineae, NE and NW, are best fit if they formed in shear in response to nonsynchronous rotation stresses, potentially as modulated by diurnal stresses. While lineae outside of Europa's ECZs can open as tension fractures, the E4 and E6 regions have been subject to minimal tensile stresses, large compressional principal stresses, and the surface's greatest differential stresses. The NE and NW oriented lineae are most consistent with an origin as conjugate shear faults, suggesting that troughs and cracks on Europa can form in shear, as well as in tension. This challenges ridge formation models that rely solely on tension to create all fractures and ridges [e.g., *Greenberg et al.*, 1998] and supports models take advantage of shear heating to aid in linear diapirism [*Head et al.*, 1999; *Gaidos and Nimmo*, 2000].

[51] A multistage history is proposed for the mapped E4 and E6 regions with the following steps: 1) early formation of ridged plains, 2) later formation of individual lineae of predominantly NW and NE orientations owing to shear failure in response to compressional principal stresses, and 3) formation of lenticulae, with continuing linea formation. The observed geological sequence suggests that pervasive development of tectonic ridged plains gave way to broader-scale regional deformation, and then to local upwelling, cryomagmatism, and/or partial melting to produce chaos and lenticulae features. A plausible interpretation of this sequence is that a brittle outer layer thickened with time and conductive heat loss processes ultimately gave way to solid-state convection and diapiric instabilities [*Pappalardo et al.*, 1998b]. In this latest stage of evolution, heat is transferred to the surface by diapiric upwelling to produce partial melting, cryomagmatism, and disruption of pre-existing terrain to form lenticulae. Such a change in Europa's geological style over a time span of only $\sim 1\%$ of the solar system's age suggests that Europa may have a cyclical history of geological activity and heat loss style [*Ojakangas and Stevenson*, 1986; *Pappalardo et al.*, 1999].

[52] **Acknowledgments.** We thank Louise Prockter, Patricio Figueroa, and the entire Galileo SSI team for their continuing productive scientific discussions and support. We thank Nicholas Sherman for his help with the original assessment of the E4 region. We also appreciate the work of all of those at JPL who made the acquisition of these images possible. This work was supported by NASA and JPL through a contract to JWH. JWH and RTP acknowledge additional support from NASA's Jupiter System Data Analysis Program. NAS acknowledges the support of a National Research Council Research Associateship at NASA Ames.

References

- Carr, M. H., et al., Evidence for a sub-surface ocean on Europa, *Nature*, 391, 363–365, 1998.
- Fagents, S. A., R. Greeley, R. J. Sullivan, R. T. Pappalardo, L. M. Prockter, and the Galileo SSI Team, Cryomagmatic mechanisms for the formation

- of Rhadamanthys Linea, triple band margins, and other low-albedo features on Europa, *Icarus*, 144, 54–88, 2000.
- Figueredo, P. H., and R. Greeley, Geologic mapping of the northern leading hemisphere of Europa from Galileo solid-state imaging data, *J. Geophys. Res.*, 105(E9), 22,629–22,646, 2000.
- Gaidos, E. J., and F. Nimmo, Tectonics and water on Europa, *Nature*, 405, 637, 2000.
- Geissler, P. E., et al., Evidence for nonsynchronous rotation of Europa, *Nature*, 391, 368–370, 1998a.
- Geissler, P. E., et al., Evolution of lineaments on Europa: Clues from Galileo multispectral imaging observations, *Icarus*, 135, 107–126, 1998b.
- Greeley, R., et al., Europa: Initial Galileo observations, *Icarus*, 135, 4–24, 1998.
- Greeley, R., et al., Geologic mapping of Europa: Overview, *J. Geophys. Res.*, 105(E9), 22,559–22,578, 2000.
- Greenberg, R., and S. T. Weidenschilling, How fast do the Galilean satellites spin?, *Icarus*, 58, 186–196, 1984.
- Greenberg, R., P. Geissler, G. Hoppa, B. R. Tufts, D. Durda, R. Pappalardo, J. Head, R. Greeley, R. Sullivan, and M. Carr, Tectonic processes on Europa: Tidal stresses, mechanical response, and visible features, *Icarus*, 135, 64–78, 1998.
- Greenberg, R., G. V. Hoppa, B. R. Tufts, P. Geissler, J. Riley, and S. Kadel, Chaos on Europa, *Icarus*, 141, 263–286, 1999.
- Head, J. W., and R. T. Pappalardo, Brine mobilization during lithospheric heating on Europa: Implications for formation of chaos terrain, lenticulae texture, and color variations, *J. Geophys. Res.*, 104, 27,143–27,156, 1999.
- Head, J. W., N. D. Sherman, R. T. Pappalardo, R. Greeley, R. Sullivan, D. Senske, A. McEwen, and the Galileo Imaging Team, Geologic history of the E4 region of Europa: Implications for ridge formation, cryovolcanism and chaos formation, *Lunar Planet. Sci.* [CD-ROM], XXX, abstract 1412, 1998a.
- Head, J. W., N. D. Sherman, R. T. Pappalardo, C. Thomas, R. Greeley, and the Galileo SSI Team, Cryovolcanism of Europa: Evidence for the emplacement of flows and related deposits in the E4 region (5°N, 305°W) and interpreted eruption conditions, *Lunar Planet. Sci.* [CD-ROM], XXX, abstract 1491, 1998b.
- Head, J. W., R. T. Pappalardo, and R. S. Sullivan, Europa: Morphological characteristics of ridges and triple bands from Galileo data (E4 and E6) and assessment of a linear diapirism model, *J. Geophys. Res.*, 104, 24,224–24,235, 1999.
- Helfenstein, P., and E. M. Parmentier, Fractures on Europa: Possible response of an ice crust to tidal deformation, *Proc. Lunar Planet. Sci. Conf. 11th*, 1987–1988, 1980.
- Helfenstein, P., and E. M. Parmentier, Patterns of fracture and tidal stress on Europa, *Icarus*, 53, 415–430, 1983.
- Helfenstein, P., and E. M. Parmentier, Patterns of fracture and tidal stresses due to nonsynchronous rotation: Implications for fracturing on Europa, *Icarus*, 61, 175–184, 1985.
- Hoppa, G. V., B. R. Tufts, R. Greenberg, and P. Geissler, Strike-slip faults on Europa: Global shear patterns driven by tidal stress, *Icarus*, 141, 287–298, 1999a.
- Hoppa, G. V., B. R. Tufts, R. Greenberg, and P. E. Geissler, Formation of cycloidal features on Europa, *Science*, 285, 1899–1902, 1999b.
- Hoppa, G. V., R. Greenberg, B. R. Tufts, P. Geissler, C. Phillips, and M. Milazzo, Distribution of strike-slip faults on Europa, *J. Geophys. Res.*, 105(E9), 22,617–22,627, 2000.
- Kadel, S. D., S. A. Fagents, R. Greeley, J. E. Klemaszewski, J. M. Moore, R. J. Sullivan, R. Greenberg, G. Hoppa, R. Tufts, and the Galileo SSI Team, Doublet ridges on Europa: Physical characteristics and origin inferred from morphology, *Eos Trans. AGU*, 79(17), Spring Meet. Suppl., S203, 1998.
- Kadel, S. D., F. C. Chuang, R. Greeley, J. M. Moore, and the Galileo SSI Team, Geological history of the Tyre region of Europa: A regional perspective on European surface features and ice thickness, *J. Geophys. Res.*, 105(E9), 22,657–22,669, 2000.
- Kattenhorn, S. A., Evidence for two complete nonsynchronous rotations of Europa's outer crust, *Geol. Soc. Am. Abstr. Programs*, 32(7), abstract 51556, 2000.
- Kraft, M. D., and R. Greeley, Ridge orientations on Europa: Observations from Galileo images, *Geol. Soc. Am. Abstr. Programs*, 29(7), A405, 1997.
- Leith, A. C., and W. B. McKinnon, Is there evidence for polar wander on Europa?, *Icarus*, 120, 387–398, 1996.
- Lucchitta, B. K., and L. A. Soderblom, The geology of Europa, in *Satellites of Jupiter*, edited by D. Morrison, pp. 521–555, Univ. of Ariz. Press, Tucson, 1982.
- McEwen, A. S., Tidal reorientation and the fracturing of Jupiter's moon Europa, *Nature*, 321, 49–51, 1986.
- Melosh, H. J., Global tectonics of a despun planet, *Icarus*, 31, 221–243, 1977.
- Melosh, H. J., Tectonic patterns on a tidally distorted planet, *Icarus*, 43, 334–337, 1980.
- Ojakangas, G. W., and D. J. Stevenson, Episodic volcanism of tidally heated satellites with application to Io, *Icarus*, 66, 341–358, 1986.
- Ojakangas, G. W., and D. J. Stevenson, Polar wander of an ice shell on Europa, *Icarus*, 81, 242–270, 1989.
- Pappalardo, R. T., Upwarped domes on Europa: Constraints on mottled terrain formation (abstract), *Lunar Planet. Sci.* [CD-ROM], XXXI, abstract 1719, 2000.
- Pappalardo, R. T., et al., Geological evidence for solid-state convection in Europa's ice shell, *Nature*, 391, 365–368, 1998a.
- Pappalardo, R. T., N. D. Sherman, J. W. Head, G. C. Collins, R. Greeley, R. J. Sullivan, and the Galileo Imaging Team, Classification of European troughs and ridges, *Lunar Planet. Sci.* [CD-ROM], XXX, abstract 1859, 1998b.
- Pappalardo, R. T., et al., Does Europa have a subsurface ocean? Evaluation of the geological evidence, *J. Geophys. Res.*, 104, 24,015–24,056, 1999.
- Prockter, L. M., A. Antman, R. T. Pappalardo, J. W. Head, and G. C. Collins, Europa: Stratigraphy and geological history of the anti-Jovian region from Galileo E14 solid-state imaging data, *J. Geophys. Res.*, 104(E7), 16,531–16,540, 1999.
- Riley, J., G. V. Hoppa, R. Greenberg, B. R. Tufts, and P. Geissler, Distribution of chaotic terrain on Europa, *J. Geophys. Res.*, 105(E9), 22,599–22,616, 2000.
- Spaun, N. A., J. W. Head III, R. T. Pappalardo, and the Galileo Imaging Team, Geological history, surface morphology, and deformation sequence in an area near Conamara Chaos, Europa, *Lunar Planet. Sci.* [CD-ROM], XXX, abstract 1899, 1998a.
- Spaun, N. A., J. W. Head, G. C. Collins, L. M. Prockter, and R. T. Pappalardo, Conamara Chaos Region, Europa: Reconstruction of mobile polygonal ice blocks, *Geophys. Res. Lett.*, 25(23), 4277–4280, 1998b.
- Spaun, N. A., L. M. Prockter, R. T. Pappalardo, G. C. Collins, A. Antman, R. Greeley, and the Galileo SSI Team, Spatial distribution of lenticulae and chaos on Europa, *Lunar Planet. Sci.* [CD-ROM], XXX, abstract 1847, 1999a.
- Spaun, N. A., J. W. Head, R. T. Pappalardo, and the Galileo SSI Team, Chaos and lenticulae on Europa: Structure, morphology, and comparative analysis, *Lunar Planet. Sci.* [CD-ROM], XXX, abstract 1276, 1999b.
- Spaun, N. A., J. W. Head, and R. T. Pappalardo, The spacing distances of chaos and lenticulae on Europa, *Lunar Planet. Sci.* [CD-ROM], XXX, abstract 1723, 2002.
- Turtle, E. P., H. J. Melosh, and C. B. Phillips, European ridges: Tectonic response to dike intrusion, *Eos Trans. AGU*, 79(17), Spring Meet. Suppl., S203, 1998.
- Zahnle, K., Cratering rates on Europa, *Lunar Planet. Sci.* [CD-ROM], XXXII, abstract 1699, 2001.

J. W. Head, Department of Geological Sciences, Brown University, Box 1846, Providence, RI 02912, USA.

R. T. Pappalardo, Astrophysical and Planetary Sciences Department, LASP, University of Colorado, Campus Box 392, Boulder, CO 80309-0392, USA.

N. A. Spaun, NASA Ames Research Center, MS 245-3, Moffett Field, CA 94035, USA. (nsaun@mail.arc.nasa.gov)